Postprint of: Płotka-Wasylka J., Rutkowska M., Jatkowska N., Malihe Z., Ghasem S., Kaykhaii M., Metal-Organic Frameworks in Green Analytical Chemistry, Metal-Organic Frameworks in Green Analytical Chemistry, Royal Society of Chemistry, 2023, DOI: 10.1039/9781839167485

CHAPTER 1

Metal–Organic Frameworks in Green Analytical Chemistry

JUSTYNA POTKA-WASYLKA,*[a,b] MAŁGORZATA RUTKOWSKA,[a] NATALIA JATKOWSKA,[a] MALIHE ZERAATI,[c] GHASEM SARGAZE[d] AND MASSOUD KAYKHAII[e]

[a] Department of Analytical Chemistry, Faculty of Chemistry, Gdańsk University of Technology, 80-233 Gdańsk, Poland; [b] BioTechMed Center, Gdańsk University of Technology, 80-233 Gdańsk, Poland; [c] Department of Materials Engineering, Shahid Bahonar University of Kerman, Kerman, Iran; [d] Graduate University of Advance Technology, Kerman, Iran; [e] Department of Process Engineering and Chemical Technology, Faculty of Chemistry, Gdansk University of Technology, Gdansk, Poland
*Email: juswasyl@pg.edu.pl

1.1 Introduction

In the last few years, much attention has been focused on metal–organic frameworks (MOFs), a class of coordination polymers, formed by metallic clusters and organic ligands through coordination bonds. This is due to their favourable properties such as high surface areas, high porosities, and tunable pore surfaces.[1–3] In addition, they are characterized by adequate mechanical and thermal stability. Taking into account these properties, it is not surprising that these materials have been incorporated into an impressive number of applications within different scientific fields, including analytical chemistry. Nowadays, a lot of studies are performed in which MOFs play important roles, as they may be considered as green media for many purposes. Nevertheless, the main focus of most studies is the

Metal–Organic Frameworks in Analytical Chemistry
Edited by Amirhassan Amiri and Masoud Mirzaei

Published by the Royal Society of Chemistry, www.rsc.org

optimization of the properties of MOFs or the increase in their crystallinity or crystal size in order to elucidate their crystal structure. In this way, thousands of compounds could be synthesized which often exhibit remarkable properties, making them interesting materials for diverse fields of application.[4,5] These compounds are in general assembled from separate inorganic building units, mostly cations or cationic metal-oxo clusters, and anionic or neutral organic connectors (linker molecules), most often polycarboxylates, imidazolates, or phosphonates. The obtained frameworks are of particular interest due to their porosity and the ease with which building units can often be replaced with topological equivalents.[6] The synthetic pathway in which these properties are generated has been mostly explored without limiting boundary conditions. However, there exist several reasons for which the investigation of ''green'' synthesis conditions represents a promising field of research. The main reason is given from a commercial point of view. MOFs are not yet utilized in real-life applications, because the use of cheap, renewable, and recyclable starting materials and avoiding waste while saving energy are considered to be crucial for industrial scale production.[7] In turn, this means that large scale applications of MOFs will be limited by their commercial availability and thus most likely also the sustainability of the synthesis procedure. From an academic point of view, such conditions are also of interest since they represent a hardly explored field of research which also opens up the opportunity to obtain new materials with remarkable structures and properties.

In addition to green synthesis of MOFs, it is important to utilize these materials in a sustainable way. In the case of analytical chemistry, it is significant to meet as much as possible the criteria of Green Analytical Chemistry (GAC), which puts into practice the development of methods that ensure the elimination/minimization of highly toxic chemical reagents (in particular toxic organic solvents), minimization of effluent and solid waste discharges, minimization of gas emissions, reduction of analysis time and steps, and incorporation of automation. Thus, the analytical chemistry trends are connected with the development of new sorbents and solvents, analytical methodologies, and technological aspects. Due to their unique properties, MOFs are considered as green media which can be used in sample preparation as well as separation. One of the important features of MOFs that makes them environmentally friendly adsorbents is the possibility of their regeneration and reusability. Depending on the application, type of used material, and method of regeneration, it is possible to re-use a MOF a few or even several dozen times, without significant loss in its adsorption capacity. Regeneration of a sorbent results in the reduction of both cost and energy.

Thus, taking into consideration the rapid expansion of MOF applications in the analytical chemistry area, it is important to evaluate the existing and future analytical MOF-based methods according to GAC principles. From this point of view, eco-friendly MOF-based methods should include features such as: green design and synthesis of MOFs, evaluation of toxicity issues of

MOFs, and incorporation of MOFs in GAC methods. This chapter will put particular emphasis on the efforts made towards greener synthesis of MOFs and the various routes and methods explored in this regard. In addition, their incorporation into less-harmful analytical chemistry methods is discussed.

1.2 Green Synthesis

The term ''Green Chemistry'' has been clearly defined by the IUPAC[8] and can be summarized as ''The invention, design, and application of chemical products and processes to reduce or to eliminate the use and generation of hazardous substances''. Since this is a rather broad definition, there exist twelve points which give a more descriptive idea[9] and which will be briefly discussed in the context of MOF synthesis herein. Similar discussions related to inorganic–organic hybrid materials[10] and zeolites[11] can be found in the literature. For the purpose of this review, we limited the minimum crucial parameters for the synthesis of MOFs to the inorganic metal cations used, the organic linker molecules used, the employed solvents, and the given synthesis conditions comprising temperature, pressure, and a suitable reactor (Figure 1.1).

Here are some rules that should be followed:

1. ''It is better to prevent production of waste rather than to treat or clean-up waste after it is formed''. The largest amount of waste for MOF synthesis is contributed by the solvents used for their synthesis and purification (or ''activation''). Thus reduction of the amount of solvent and especially replacement with a ''greener'' solvent are highly desirable.[7]

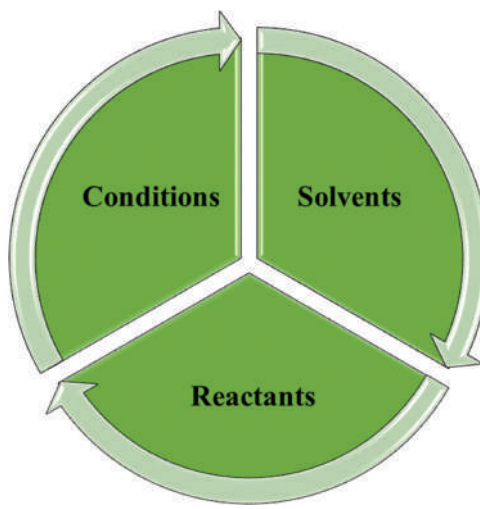

Figure 1.1 Crucial parameters for green MOF synthesis.

2. ''Synthetic methods should be designed to maximize the incorporation of all materials used in the process to the final product''. Regarding MOFs, this point simply favours high-yield synthesis over low-yield synthesis and again refers to the amount of utilized solvent. Any by-product or waste which is formed must be subjected to post-treatment procedures, thus increasing time and energy consumption.
3. ''Whenever practicable, synthetic methodologies should be designed to use and generate substances that possess little or no toxicity to human health and to the environment''. In the synthesis of MOFs this can be often taken into account regarding the counterion of the metal salt employed. This combined with point 1 recommends the use of hydroxides or oxides as sources of metal ions, because when they combine with protons generated from the acidic linker molecules, only water is formed as a by-product. This also means that solvents which decompose into hazardous products during synthesis should preferably not be used. The typically employed dimethylformamide (DMF) is not only a hazardous chemical itself, but is also able to easily form dimethylamine upon hydrolysis, which also poses challenges in terms of handling and disposal.[12]
4. ''Chemical methods should be designed to preserve efficacy of function while reducing toxicity''. Even if a green preparative pathway can be developed for a certain MOF, the product must still exhibit the desired properties. The synthesis route might alter the properties of the products obtained; for example, the presence of structural defects or the crystal size and shape.
5. ''The use of auxiliary substances (*e.g.* solvents, separation agents, *etc.*) should be made unnecessary whenever possible and innocuous when used''. Synthesis without a solvent has hardly been reported;[13] minimization of the amount is nevertheless possible, for example, by liquid assisted grinding.[14] Considering the solvent used for purification of a crude MOF as an auxiliary substance, this means that regarding its sustainability, sometimes elaborate activation procedures strongly affect the characteristics of the preparation. Moreover, this point can be once more related to the use of harmless solvents like water.
6. ''Energy requirements should be recognized for their environmental and economic impacts and should be minimized. Synthetic methods should be conducted at ambient temperature and pressure''. The latter emphasizes especially the risks associated with solvothermal synthesis. Albeit a considerably safe method in the laboratory, pressurized conditions pose severe challenges on the production of larger amounts of a material. Since only a very few examples report MOF synthesis at room temperature, the synthesis under reflux conditions can be considered a realistic goal. Lowering of the energy consumption can be mostly achieved by not only synthesis at temperatures which are as low as possible but also employing alternative methods of energy application like ultrasound and mechanochemistry.

7. ''A raw material or feedstock should be renewable rather than depleting wherever technically and economically practicable''. The organic building units in MOFs are mostly substances used in polymer chemistry (*e.g.*, phthalates) and thus do not represent a renewable feedstock. It is therefore highly desirable to use linker molecules that can be obtained from renewable sources like starch and cellulose.[15] Identical conclusions can be drawn for the solvent and thus water and organic solvents produced from renewable feedstock like ethanol should be preferably used.
8. ''Unnecessary derivatization (blocking group, protection/deprotection, temporary modification of physical/chemical processes) should be avoided whenever possible''. While it is easier to apply this in organic synthesis, there is also some relevance for MOFs at this point. Since the organic building units can also be utilized as non-protic reactants, for example, as esters of carboxylic acids,[16] this recommends the use of simpler protic precursors to avoid additional waste and synthesis steps.
9. ''Catalytic reagents (as selective as possible) are superior to stoichiometric reagents''. In a few cases it could be shown that minute amounts of solvent suffice for the preparation of a MOF. Thus considering the solvent as a catalyst, such synthetic routes are highly recommended.
10. ''Chemical products should be designed so that at the end of their function they do not persist in the environment and break down into innocuous degradation products''. MOFs are not yet used in real-life applications, which is mainly due to their degradation under working conditions, especially when used in open systems. Leaching of the components from the material would clearly inhibit the use of highly toxic building units like Pb^{2+} and Cd^{2+} ions as well as hazardous organic building units.
11. ''Analytical methods need to be further developed to allow for real time, in process monitoring and control prior to the formation of hazardous substances''. Little is known about the side products formed during MOF synthesis since the preparation is commonly carried out on a lab scale. In the future, this could become extremely relevant, especially if potentially hazardous chemicals cannot be replaced. Such process monitoring can also be employed to substantially shorten the reaction times which are often set to 12 or 24 hours for practical reasons.
12. ''Substances and the form of a substance used in a chemical process should be chosen so as to minimize the potential for chemical accidents, including releases, explosions, and fires''. This point will especially gain relevance for large scale synthesis while it has been mostly ignored up to now. An example is the typical combination of DMF with a metal nitrate during the synthesis of MOFs. This adds an oxidizing substance to a flammable substance, a combination which is reasonably dangerous and given as a potential risk in all safety data sheets.

Taking these considerations into account, the different approaches towards greener synthesis procedures for MOFs are discussed later. At the beginning, some archetypal MOFs and the most relevant groups of MOFs are discussed and how their synthesis conditions were adjusted towards sustainability and efficiency. Then, some perspectives on possible developments are given. The major challenges are typically related to the replacement of a hazardous organic solvent, mostly DMF, or the development of an alternative route starting from solvothermal synthesis conditions. The most obvious approach towards green synthesis and also the most often reported one is the change of synthetic conditions in order to fulfil at least some of the points summarized earlier. Such efforts have been made for several MOFs of interest by replacing potentially hazardous reactants with "greener" ones.[17]

1.3 Preparation of MOFs Considering GAC Principles

MOFs are prepared by different methods such as hydrothermal,[18,19] solvothermal,[20,21] electrochemical,[22,23] and slow diffusion techniques.[24] In these conventional methods, reactions are carried out for long periods and, in some cases, high temperatures and energies are needed for the progress of the reaction, which makes it difficult to control synthesis conditions. Also, the products synthesized in these methods do not have desirable physicochemical properties.

Recently, rapid methods like ultrasound and reverse micelle (RM) methods have been used, which can facilitate the performance of reactions and produce MOFs under mild conditions.[25,26] Ultrasound synthesis is a simple, rapid, low cost, environment-friendly, and safe route which accelerates the processes. When a liquid is exposed to high-intensity ultrasonic irradiation (20 kHz–10 MHz), shock waves are formed, which lead to acoustic cavitation in the medium. In the ultrasound method, different parameters are used to control various properties of products. Many researchers have investigated the chemical or physical effects of ultrasonic irradiation on several properties of MOFs.

A RM method is a simple route for preparation of materials in which RMs are organized in an organic medium which serve as nanoreactors for the formation of nanostructures.[27,28]

A typical RM method for synthesis of MOFs involves the following steps: (a) a surfactant is dissolved in an organic solvent; (b) an aqueous solution containing metal and ligand precursors is added to the surfactant solution to prepare RMs acting as nanoreactors; and (c) a MOF grows inside the micelles through the reaction of the metal precursor with ligand.[29]

In general, although some properties of MOFs produced by either the ultrasound or RM method such as thermal stability and surface area are higher than those of MOFs produced by other methods, the properties of the products are not very ideal for industrial applications.[26,30]

Furthermore, we could not find any report on the use of ultrasound assisted RM method for the synthesis of MOFs; therefore, in the case of using this novel method (which is the combination of two rapid, cost-effective, and low-energy methods), the properties of the products are expected to be considerably enhanced.[31,32]

1.3.1 Green Design and Synthesis of MOFs

Another case that should be considered about MOFs is the manner of experimental design for investigating their properties. In previous works, the effects of synthesis conditions on the properties of MOFs have been investigated using conventional experimental design methods, which could increase the number of experiments and ignore the interaction between the factors.[33,34] However, using a scientific experimental design does not impose such limitations, but leads to systematic studies. Therefore, the systematic study of the process could be as important as selecting a suitable synthesis method for introducing a new MOF compound.

1.3.1.1 Green Design

As mentioned earlier, control of the impact of the synthesis parameters on different properties of MOF samples is highly important. In earlier studies, the effects of several synthesis parameters on the properties of products have been examined using one-factor-at-a-time (OFAT) design, in which a number of parameters are assumed to be constant and one factor is varied for optimization. The OFAT design not only increases the number of experiments, but also ignores the interaction between parameters.[35] Therefore, the systematic control of products' properties is impossible using conventional designs; for example, the 2^{K-1} factorial design can be used to control products' properties.[36,37] Nevertheless, since a large number of experiments should be selected in this method, it is highly important to choose an ideal design that makes the systematic study of products possible and reduces the number of experiments. The fractional factorial design is one of the systematic ways through which the number of experiments is reduced and synthesis parameters are scientifically investigated.[36] According to the literature, no reports have been found on the use of this systematic method for controlling the properties of MOFs. Regarding the analysis of variance (ANOVA) results and their generalization to various obtained properties, the designs obtained using the 2^{K-1} factorial could be analysed. Based on the data obtained from SEM, TGA-DSC, and BET analysis, it seemed that level e had the best conditions for the synthesis of thorium-based-MOF compounds; so that, at this level, the synthesis parameters (surfactant content, ultrasound duration, temperature, and ultrasound power) were optimal and would lead to the synthesis of samples with maximum thermal stability, uniform morphology, minimum particle size, and maximum surface area. Moreover, Fourier transform infrared (FTIR) spectra showed that at this

level (e), all of the Th-MOF bonds were properly formed (Figure 1.2). Also, at level b, the particles were strictly agglomerated and their sizes were in the bulk form (Figure 1.3).[25]

Furthermore, at this level, according to the FTIR spectrum in Figure 1.2(b), the Th–O bonds were not formed; since the maximum values of the ultrasound parameters were used (Table 1.1), it seemed that this resulted in the destruction of some of the bonds in the final structure.[36] In the present work, destruction of the bonds had a considerable effect on the thermal behaviour as well as adsorption/desorption behaviours of the Th-MOF samples so that, at level b, the sample had the minimum thermal stability (Figure 1.4)[25] and surface area (Figure 1.5).[25] Moreover, the adsorption/desorption behaviours of sample b were similar to the fourth type of classical isotherms. On the other hand, at this level, since the surfactant content had the minimum value compared with the optimal level, it could have no desirable effect on various properties of sample b. Since ANOVA confirmed the importance of the interactions between the synthesis parameters, it was concluded that, at level b, these interactions would intensify the effects of the high intensity of the ultrasound parameters (which caused the destruction of bonds) and the low surfactant content values (which caused a significant reduction in various properties of the sample).[38]

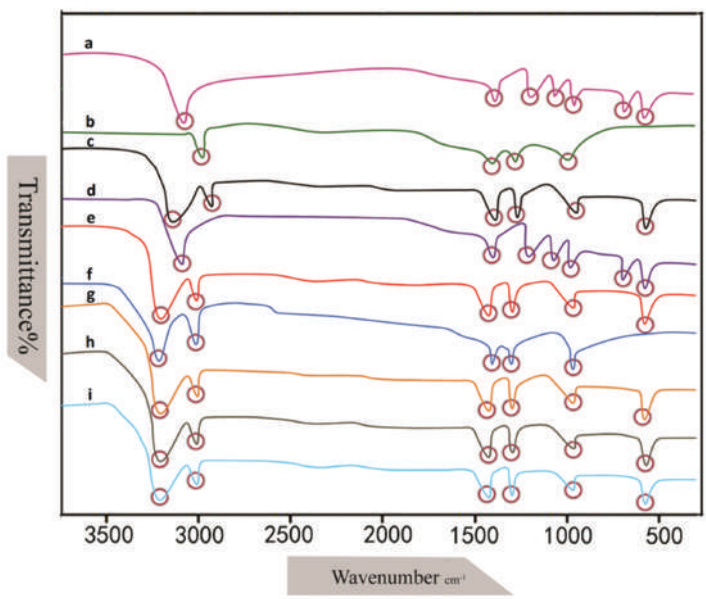

Figure 1.2 FTIR spectra of Th-MOF samples synthesized under different ultrasound assisted RM conditions (a–i). Reproduced from ref. 25 with permission from Elsevier, Copyright 2018.

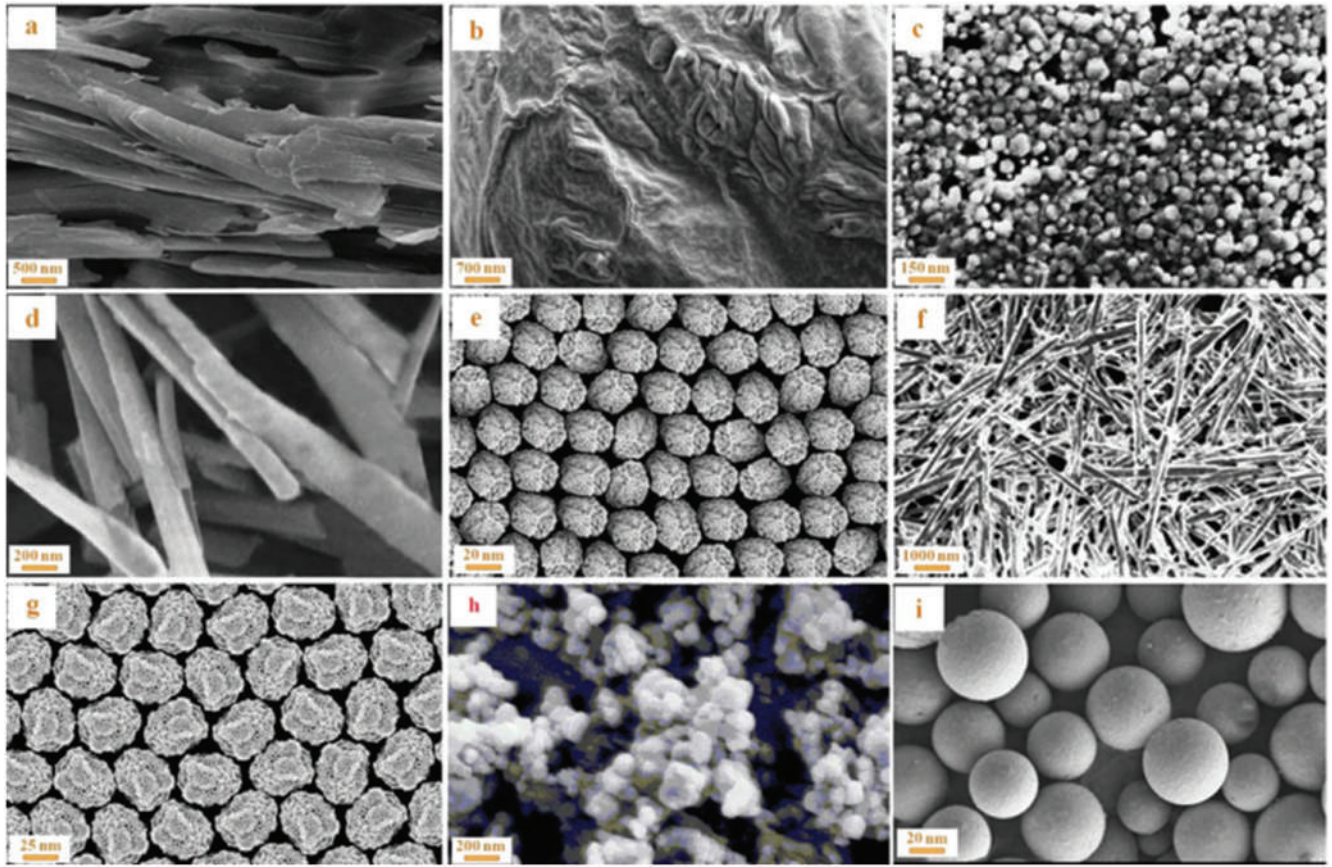

Figure 1.3 SEM micrographs of Th-MOF samples synthesized under different conditions of the ultrasound assisted RM method (a–i). Reproduced from ref. 25 with permission from Elsevier, Copyright 2018.

Table 1.1 Randomized complete 2^{K-1} factorial design for TS, SD, and SA experiments of Th-MOF samples synthesized under different conditions of the ultrasound assisted RM method.

Sample (level)	Std order	Centre Pt	A (mmol)	B (min)	C (°C)	D (W)	REP	SD (nm)	TS (°C)	SA ($m^2 g^{-1}$)
a	9	1	+1	−1	0	−1	1	217	220	0.42×10^3
							2	216	219	0.42×10^3
b	5	1	−1	+1	+1	+1	1	497	185	0.18×10^3
							2	496	185	0.18×10^3
c	6	1	0	−1	−1	+1	1	64	284	1.71×10^3
							2	65	284	1.71×10^3
d	3	1	+1	0	0	+1	1	123	257	1.10×10^3
							2	124	257	1.10×10^3
e	2	0	0	0	0	0	1	27	354	2.20×10^3
							2	27	354	2.20×10^3
f	8	1	−1	+1	+1	0	1	187	239	0.64×10^3
							2	186	239	0.64×10^3
g	4	1	0	−1	0	0	1	36	321	2.01×10^3
							2	36	320	2.01×10^3
h	7	1	−1	0	0	0	1	77	265	1.61×10^3
							2	77	266	1.61×10^3
i	1	1	0	−1	−1	0	1	40	312.6	1.92×10^3
							2	41	312.0	1.92×10^3

At level g, many of the synthesis parameters were similar to the optimal conditions; however, due to the shorter duration of irradiation, the particle size was slightly higher and the thermal stability and surface area were slightly less than the results obtained at the optimal level (e). Moreover, the adsorption and desorption behaviours of sample g were similar to those of the optimal sample (similar to the fifth-type isotherm). At levels i and c, since the ultrasound duration and temperature had minimum values, the properties of the Th-MOF samples were slightly reduced compared with those under the optimal conditions and the isothermal behaviours were similar to the first-type isotherm, which could be the reason for the microdistribution of the pores. At level c, besides the low values of the ultrasound duration and temperature parameters, since the value of ultrasound power was higher than the optimal value (negative effect due to the high intensity), this factor caused a slight difference between samples c and i in terms of the obtained properties. The FTIR spectra in Figure 1.2 showed that the bonds associated with the formation of Th-MOFs were formed properly in samples i and c. Based on the ANOVA results, the surfactant content was selected as an important factor affecting the properties of Th-MOF samples; therefore, it was expected that selecting its appropriate amount would lead to the improvement of various properties of the products.[39,40] However, at level h, despite selecting the optimal values for the ultrasound parameters, since the surfactant content was lower than that at the optimal level, the thermal stability (Figure 1.4) and surface area (Figure 1.5) of sample h were reduced. According to the SEM image in

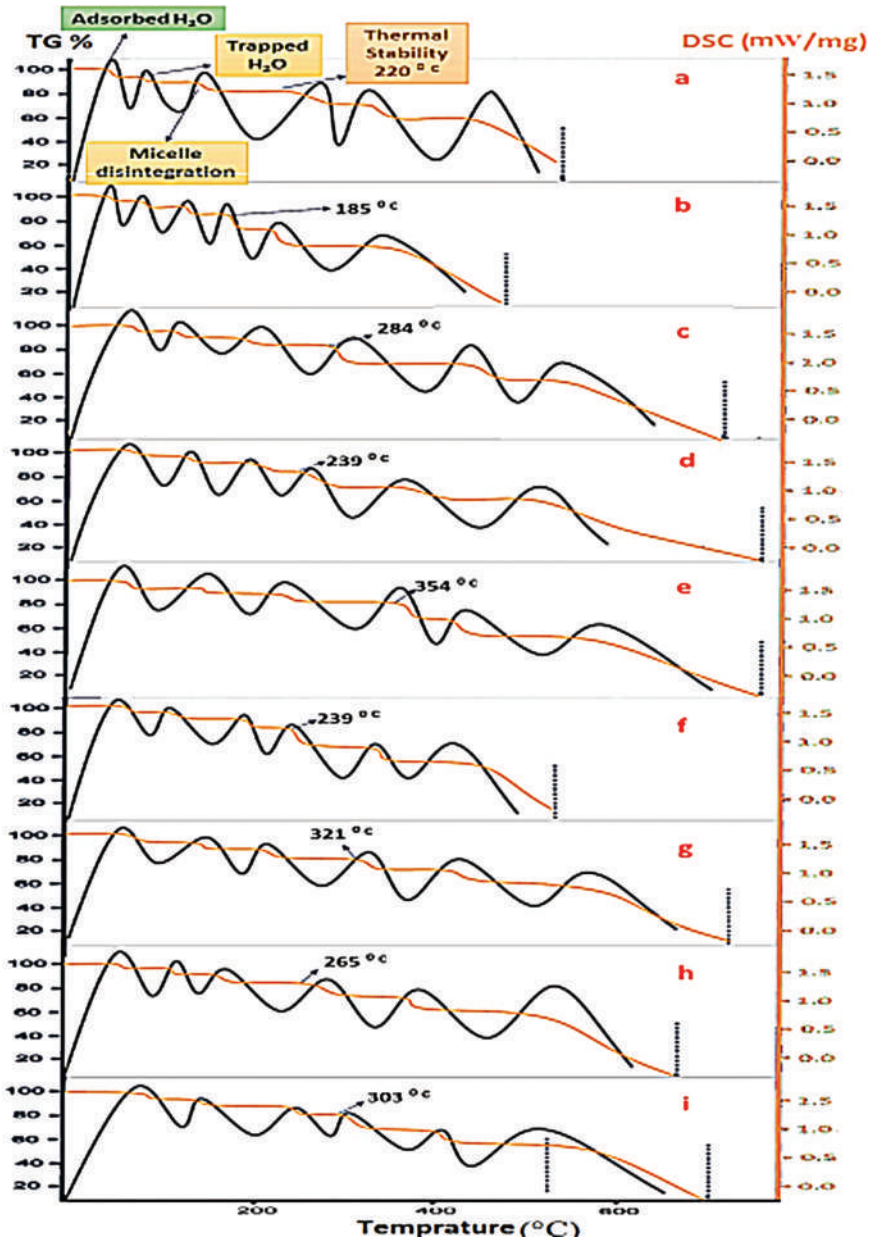

Figure 1.4 Thermal behaviours of Th-MOF samples synthesized under different conditions of the ultrasound assisted RM method (a–i). Reproduced from ref. 25 with permission from Elsevier, Copyright 2018.

Figure 1.3, the particles were partly aggregated together at level h. Compared with level h, at level d, the surfactant content selected was higher than the optimal value, causing the surfactant to react with the Th-MOF sample, instead

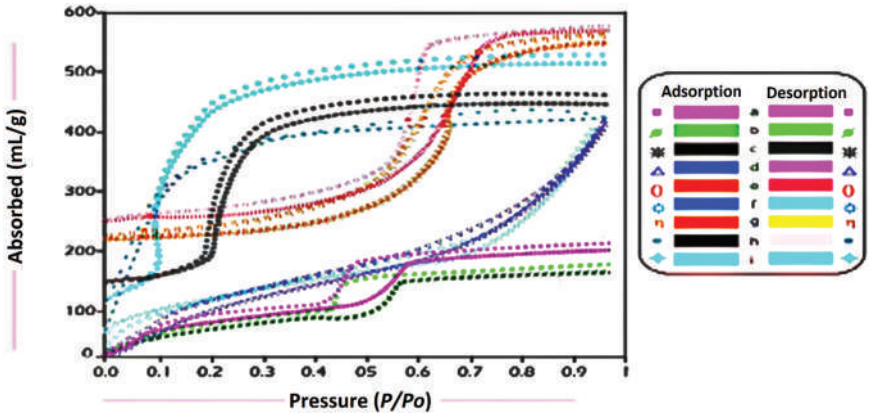

Figure 1.5 Adsorption/desorption isotherms of Th-MOF samples synthesized under different conditions of the ultrasound assisted RM method (a–i). Reproduced from ref. 25 with permission from Elsevier, Copyright 2018.

of improving the properties of the product. As a result, the morphology of sample d was in the form of a rod (Figure 1.3) with an average width of 123 nm, and its thermal stability and surface area were reduced compared to samples e, g, i, c, and h. TG and DSC analyses showed that, in sample d, the micelle disintegration temperature was increased (Figure 1.4), which could indicate the surfactant self-assembly. Figure 1.3(d) shows the FTIR spectrum of sample d. According to this spectrum, the frequencies near 1092.91 cm^{-1} for S=O and 694.24 cm^{-1} for S–O bonds confirmed the occurrence of the surfactant self-assembly at level d. At level f, first, the surfactant content was lower than that at the optimal level (e); second, the values of ultrasound duration and temperature selected were so high that the Th–O bond (Figure 1.2) was not formed properly (resulting in the destruction of the bond). Consequently, according to Figure 1.3, these factors resulted in the formation of belts with an average width of 187 nm and aggregation of the particles due to the instability caused by the destruction of the Th–O bond in sample f. Furthermore, according to Figures 1.4 and 1.5, the thermal stability and surface area of level f were strictly reduced compared with those of the optimal level. At level a, as level d, selecting high surfactant content values led to the occurrence of the surfactant self-assembly.[41] However, since the parameters of ultrasound duration and power at level a selected were at the minimum value compared with those at the optimal level and also due to the interaction between the factors (ANOVA results), the thermal stability and surface area of sample a were significantly reduced compared with those of sample d and the morphology of the product was such that the particles were agglomerated and their sizes were considerably increased.

Figure 1.6 shows the XRD patterns of samples a–i under various synthesis conditions of the ultrasound assisted RM method.[25] Based on these

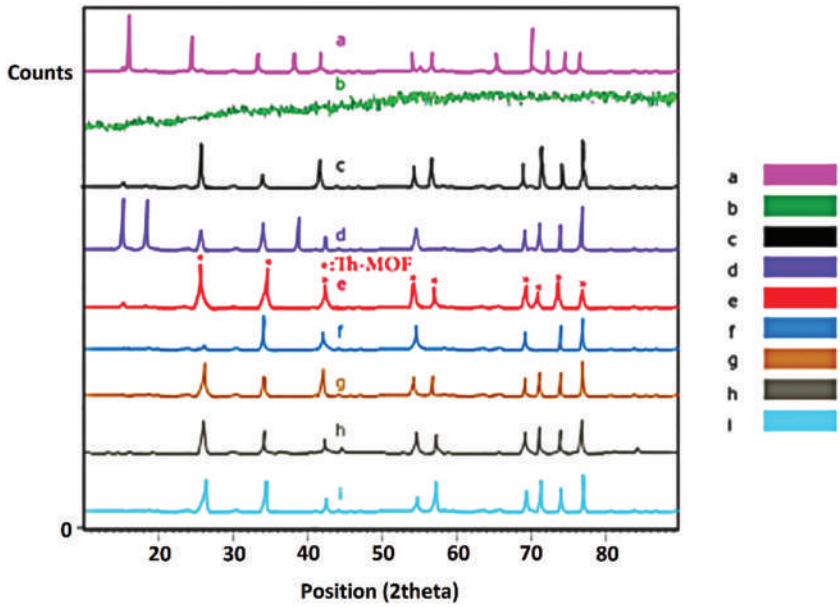

Figure 1.6 XRD patterns of Th-MOF samples synthesized under different ultrasound assisted RM conditions (a–i). Reproduced from ref. 25 with permission from Elsevier, Copyright 2018.

patterns, at level e, the product had wide peaks related to the formation of the Th-MOF sample; these peaks indicated that the structure was of nanometric dimensions. At level b, the sample had an amorphous structure, which could be due to the destruction of the bonds caused by the high intensity of the ultrasound parameters as well as the low value of the surfactant content (compared to the optimal level).[35] For samples a and d, more peaks can be seen than for samples c, i, e, f, g, and h, indicating the surfactant self-assembly, which was consistent with the FTIR spectral results. At level f, due to the high values of ultrasound duration and temperature, some of the thorium MOF-related XRD patterns were not formed, while at other levels, the XRD patterns related to the formation of Th-MOF were formed properly, except that based on the difference between the sizes of crystals, widening of the peaks was different from each other.

The use of novel organic materials with several acidic compounds requires optimizing the synthesis conditions to identify the effective parameters and to investigate them by a number of statistical methods. As a result, the Taguchi approach is one of the well-known methods for the design of experiments (DOE).[42] Simulation is also performed to investigate the mechanism of Cu-MOF synthesis. The Taguchi method, first developed by Genichi Taguchi, is an optimization method to minimize the time and cost of an experiment.[43] This method uses orthogonal arrays to organize the parameters more effectively and determines the levels of parameter

change. Since the Taguchi method is classified as a fractional factorial design method, fewer experiments are needed to achieve similar results to the complete factorial design.[37,44,45] In the Taguchi method, different experimental conditions are tested in an orthogonal array with the aim of reducing experimental errors and process changes, enhancing the process efficiency and optimizing the set of dominant parameters.[46] Signal-to-noise (S/N) ratio analysis is crucial for finding optimal conditions. Smaller-is better, larger-is-better, and nominal-is-best S/N ratios are the three common types of S/N ratios for optimization problems. The S/N ratio for nominal-is-best characteristics can be expressed according to eqn (1.1).[47]

$$\mathrm{S/N} = -10 \times \log\left(\sum_{i=1}^{n}\left(\frac{1}{y_i}\right)^2 \Big/ n\right) \tag{1.1}$$

where n represents the number of replicates under the same experimental conditions and y_i is obtained for the target value in each experiment. Table 1.2 summarizes the details of each experiment. It is worth noting the number of trials using the Taguchi design. Minitab software was used to design the test matrix and for analysis of variance (ANOVA).

Table 1.3 summarizes 16 independent experiments designed using the Taguchi method and the S/N ratio associated with each experiment. All samples were analysed in terms of BET surface areas calculated. Each experiment was also repeated twice and used to calculate S/N ratio using eqn (1.1). By subtracting the maximum S/N ratio from its minimum value across the four levels, the importance of each control factor can be determined. The factor that has the least difference in the S/N ratio has a less significant role in controlling the synthesis process.[48]

It can be concluded from Table 1.4 that the effect of the reactant ratio (extract/$CuNO_3$) is more significant than those of the other factors. The importance of the control factors can be stated in ascending order: temperature < reactant ratio < feed rate < reaction time.

Figure 1.7 shows the S/N ratio against each of the controlling factors; the optimal conditions for the synthesis of Cu-MOF were as follows:[37] a reactant ratio (extract/$CuNO_3$) of 2.5, a feed rate of 1 mL min^{-1}, a temperature of 85 °C, and a reaction time of 90 min.[37]

Table 1.2 Selected controlling factors and their levels.

	Levels			
Controlling factors	1	2	3	4
Reactant ratio (extract/$CuNO_3$)	1	1.5	2	2.5
Temperature (°C)	65	75	85	95
Reaction time (min)	65	75	85	95
Feed rate (mL min^{-1})	1	2	3	4

Table 1.3 The experimental design with computed selectivity and their corresponding S/N ratios.

	Controlling factors					
No.	Reactant ratio (extract/$CuNO_3$)	Reaction time (min)	Temperature (°C)	Feed rate ($mL\,min^{-1}$)	BET surface area ($m^2\,g^{-1}$)	S/N ratio
1	1	65	45	1	946	59.51
2	1	75	60	2	302	49.6
3	1	85	75	3	220	46.84
4	1	95	90	4	859	52.88
5	1.5	65	60	3	441	58.67
6	1.5	75	45	4	12.04	54.88
7	1.5	85	90	1	1204	10.75
8	1.5	95	75	2	555	21.61
9	2	65	75	4	1172	61.37
10	2	75	90	3	33	45.34
11	2	85	45	2	1642	30.37
12	2	95	60	1	2416	64.3
13	2.5	65	90	2	2322	67.31
14	2.5	75	75	1	1965	65.86
15	2.5	85	60	4	185	66.44
16	2.5	95	45	3	2100	67.66

Table 1.4 Calculated S/N ratios and the contribution of each controlling factor.

Level	Reactant ratio (extract/$CuNO_3$)	Temperature (°C)	Reaction time (min)	Feed rate ($mL\,min^{-1}$)
1	33.66	40.28	32.97	43.66
2	27.75	21.86	33.87	39.03
3	35.93	34.53	37.25	29.14
4	41.24	41.92	34.49	26.75
Delta	13.49	20.06	4.27	16.91

1.3.1.2 Green Synthesis

The ultrasound assisted microwave (UAMw) and microwave (Mw) methods have advantages such as high-speed production, low cost, and eco-friendliness and they can be performed at ambient temperature and pressure.[49,50] In these methods, compounds with a variety of structures and different physicochemical properties are synthesized by controlling synthesis conditions.[51] The use of such effective methods, compared to other conventional methods, results in products with some better properties. However, some other reports mentioned that MOF samples have low specific surface area and bulk size particles.[52,53]

Figure 1.8 shows the XRD patterns of the Ta-MOF samples with high crystallinity, which are synthesized using the Mw and UAMw methods.[54] Based on the Debye–Scherrer equation, the crystal sizes of both samples are in the nanometric range;[55] however, the sample synthesized by the UAMw method has smaller crystals due to showing wider peaks (22 nm in the UAMw method compared to 56 nm in the Mw method). Since the samples

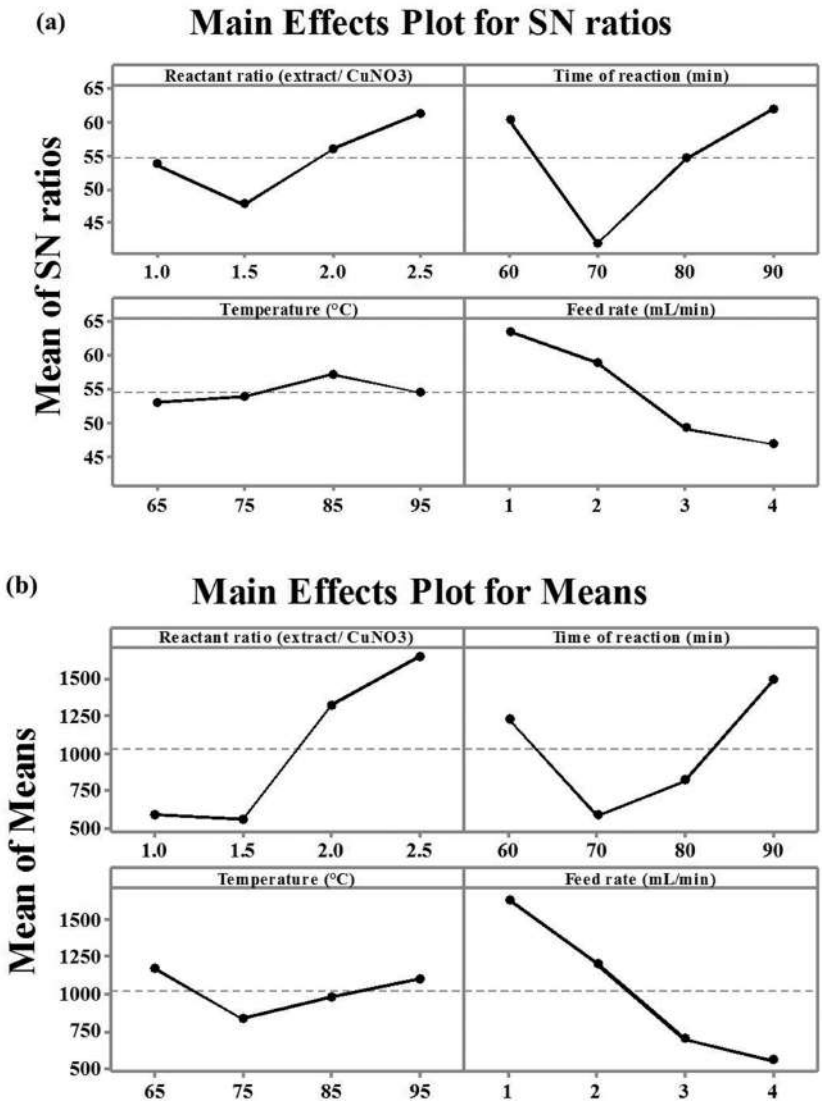

Figure 1.7 (a) Average S/N ratios and (b) mean at four levels for each parameter. Reproduced from ref. 37, https://doi.org/10.3389/fchem.2021.722990, under the terms of the CC BY 4.0 license, https://creativecommons.org/licenses/by/4.0/.

are synthesized under two different conditions, it is possible that the synthesis parameters would have a great effect on the size of crystals. In both the Mw and UAMw methods, the corresponding XRD patterns were indexed to the monoclinic crystal system of the pure complex of $C_{21}H_{14}N_3O_{13}Ta$ with the space group $P21/n$ and unit cell parameters of $a = 12.986$ Å, $b = 8.9104$ Å, $c = 24.942$ Å, and $\alpha = 90.049^{\circ}$.

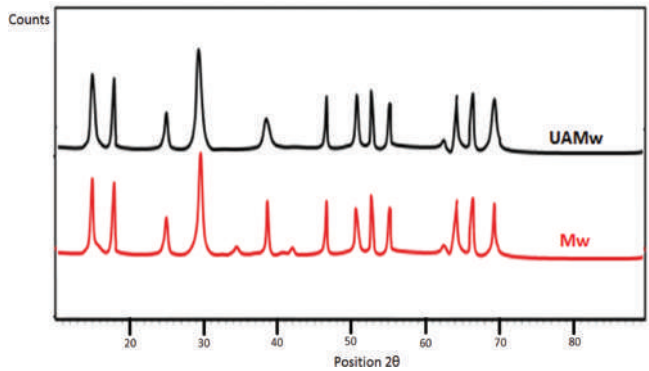

Figure 1.8 The XRD patterns of the Ta-MOF samples synthesized by the two different methods (Mw and UAMw). Reproduced from ref. 54 with permission from Springer Nature, Copyright 2018.

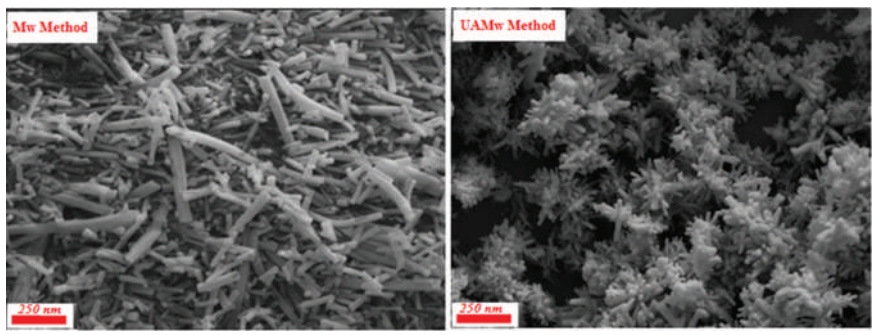

Figure 1.9 The SEM images of the Ta-MOF samples synthesized by the Mw and UAMw methods. Reproduced from ref. 54 with permission from Springer Nature, Copyright 2018.

Figure 1.9 shows the SEM images of the Ta-MOF samples synthesized under optimal conditions of the Mw and UAMw methods.[56] Based on the results, the morphology of the sample synthesized by the Mw method is rod-shaped with an average diameter of 76 nm; however, using the UAMw method produces nanoparticles (NPs) with a flower-like morphology. The sample synthesized by the UAMw method has a more uniform morphology than that synthesized by the Mw method; accordingly, no evidence of agglomeration and aggregation of particles can be found while using the UAMw method. However, in the Mw method, the particles are partially aggregated, which can increase the diameter of the Ta-MOF sample.

It is important to exploit and commercialize MOF production methods that are sustainable, mass-produced, and cost-effective.[56,57] Therefore, green synthesis is required to make MOFs by using non-toxic and efficient materials:[58,59] for example, using water for the green synthesis of MOFs, because water is more accessible and vibrant than organic solvents. However,

the important point here is that most of the water-soluble organic bonds are weak and cause MOFs to be unstable.[60,61] This method may hence not be suitable for mass production, but the time which is required for the MOF synthesis, involving metal ion bonding, is significantly shorter than the other methods. In these methods, the water-solubility issues have been mitigated mainly by using sodium salts of the organic linkers and by increasing the length of the tubing systems to increase the overall reaction time.[62–64]

Using the extract of *Satureja hortensis*, an Al-MOF was synthesized, and Figure 1.10(a) and (b) presents the TEM images of the Al-MOF with CA and Na2-CA, respectively, with a spherical shape and high porosity.[65] Considering the surface area as a criterion, the fraction of pores (dark area) to the total surface in the TEM image was estimated using image analyser software. As shown in Figure 1.10(c) and (d),[65] the background is blue and the pore phase is red and green, with phase percentages of samples S1 and S2 of 70% and 83%, respectively.[66]

Figure 1.11 shows the N_2 desorption/desorption isotherms of S1 and S2.[65] The difference between the two isotherms indicates the distinct nature of the two samples in terms of textural properties. There is also a different

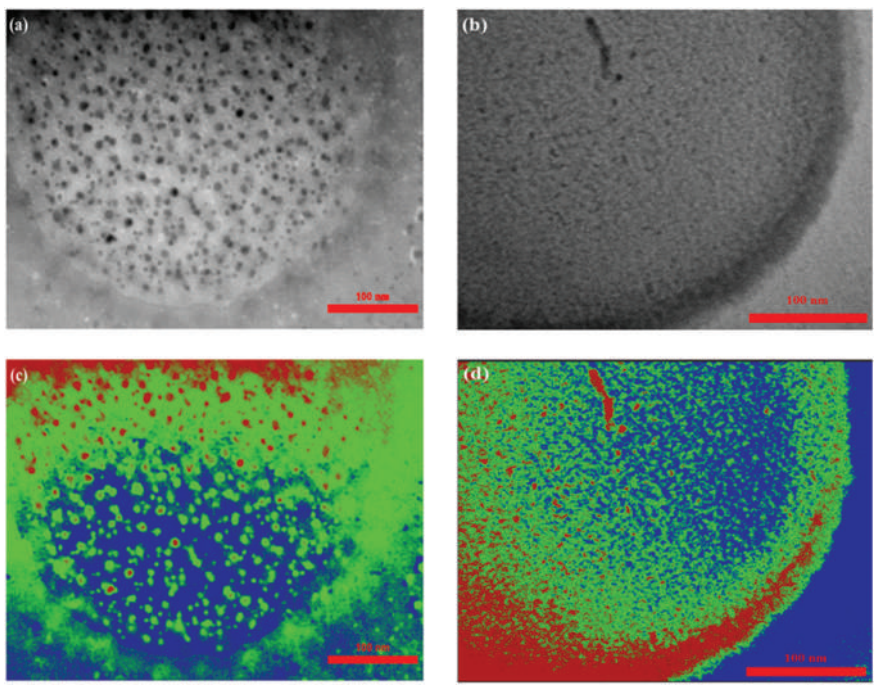

Figure 1.10 TEM images of the Al-MOF with CA and Na2-CA such as (a) S1 and (b) S2, and (c and d) TEM image analysis, respectively. Reproduced from ref. 65, https://doi.org/10.3389/fchem.2021.784461, under the terms of the CC BY 4.0 license, https://creativecommons.org/licenses/by/4.0/.

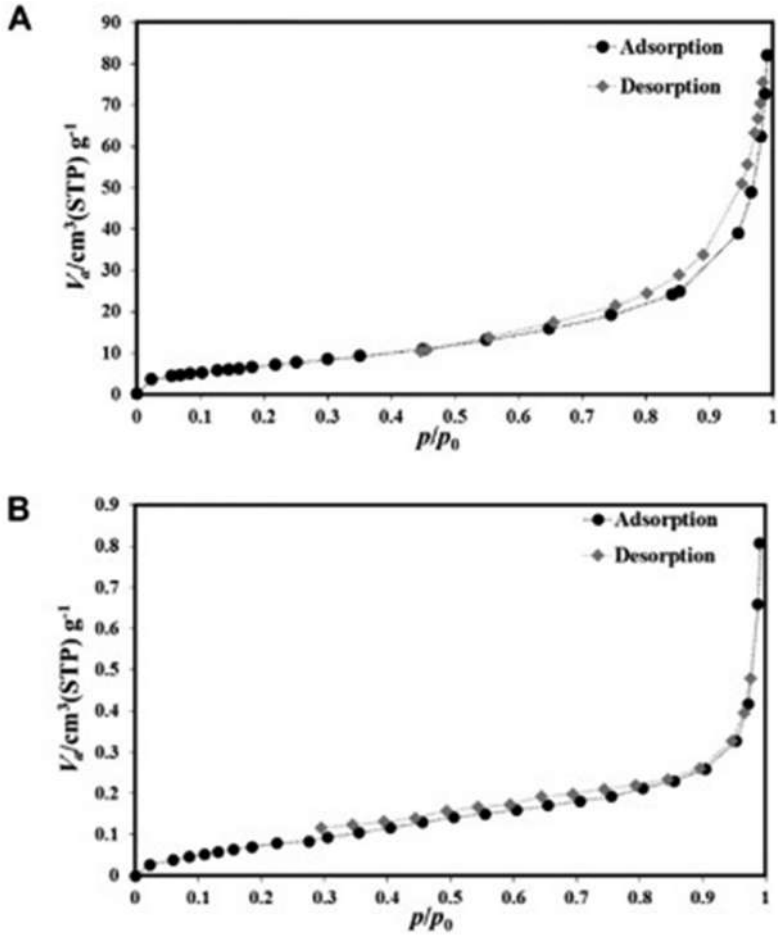

Figure 1.11 BET technique of the N_2 adsorption/desorption isotherms of the (A) S1 and (B) S2 samples. Reproduced from ref. 65, https://doi.org/10.3389/fchem.2021.784461, under the terms of the CC BY 4.0 license, https://creativecommons.org/licenses/by/4.0/.

hysteresis cycle depicted in Figure 1.11, ending in sample S1 at $p/p_0 = 0.45$ and sample S2 at $p/p_0 = 0.3$. The larger hysteresis cycle of sample S1 is attributed to the presence of guest molecules in the pores.[66,67] Figure 1.12 shows the pore size distribution of S1; the average value was 20 nm.[65] While the sample S2 pore size distribution was <20 nm, the average value was 12 nm. The surface areas of the prepared S1 and S2 samples were estimated using BET analysis (Figure 1.11). As shown, the adsorption isotherms of both samples are similar to the type III isotherm,[68] while the average surface areas of samples S1 and S2 were 1245.2 $m^2 g^{-1}$ and 2452.8 $m^2 g^{-1}$, respectively. The high surface areas for the samples can be attributed to the select novel synthesis route as well as the optimization process. Accordingly, the

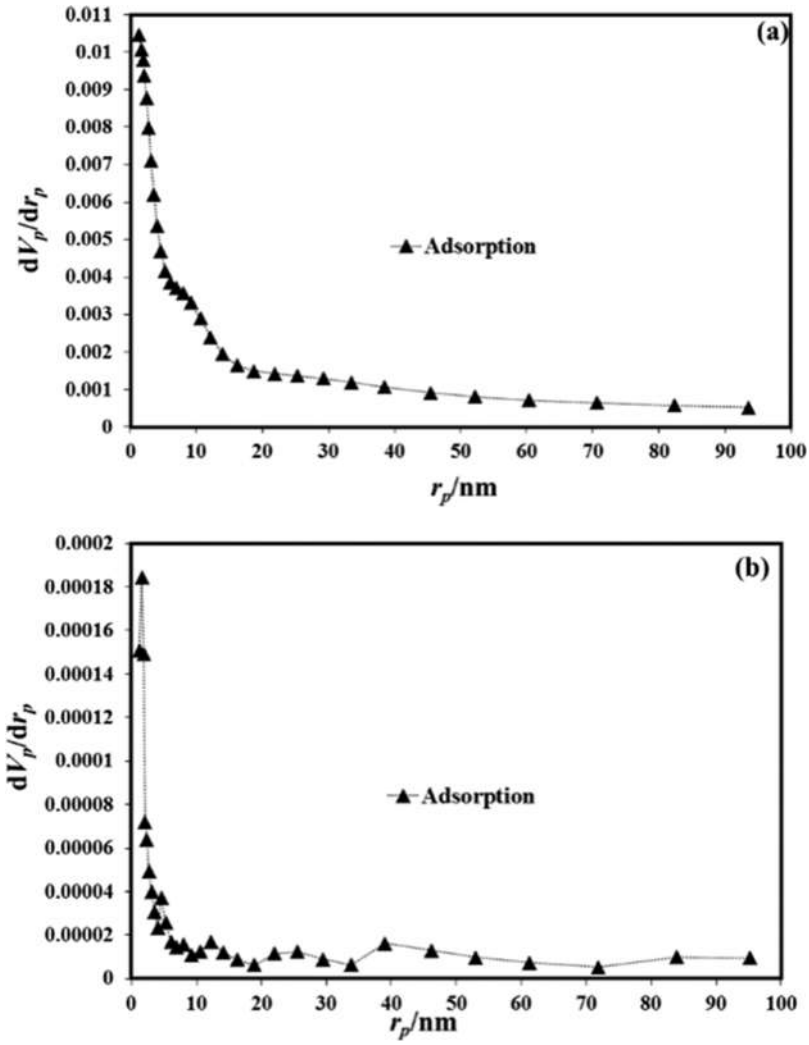

Figure 1.12 The pore size distributions of the (a) S1 and (b) S2 samples with the BJH method. Reproduced from ref. 65, https://doi.org/10.3389/fchem.2021.784461, under the terms of the CC BY 4.0 license, https://creativecommons.org/licenses/by/4.0/.

prepared Al-MOF was accepted as a mesoporous martial as reported by Moreno *et al.*[69] The decrease in surface area compared to previous reports is probably due to the presence of organic extract molecules that are not completely removed by activation. In addition, the molecules of solvent trapped in the MOF pores reduce the specific surface area. On the other hand, Al-MOF powders have been agglomerated and the gas penetration does not occur completely.[68,69]

As an application, Al-MOFs were applied for the treatment of breast cancer cells and they seem to be more effective against the proliferation of these cells when compared with herbal extraction.[70]

1.4 Properties of MOFs Towards GAC

Throughout the years, MOFs have been recognized for their fascinating properties, including their large specific surface area, enormous porosity (up to 90% free volume), low density, and unique structure.[71] One of the unique characteristics of MOFs compared to other porous materials such as zeolites and carbons is their tunability. By selecting different combinations of Secondary Building Units (SBUs) and controlling the experimental conditions (pH, concentration, temperature, and time), the pore volume, size, surface area, and crystallite size of MOFs can be tuned as expected, which significantly expands their range of applications and improves their efficiency in given applications. In addition, MOFs can be post-synthetically modified to enhance their properties. By functionalization in the pores or outer surface with different functional groups, it is possible to use MOFs for the adsorption of different analytes through H-bonding and hydrophilic–hydrophobic interactions.[72,73] Due to this tunability, more than 80 000 MOFs have already been characterized.[74] In light of their advantageous features, this class of materials has attracted considerable attention in analytical chemistry for some time, especially for their use as adsorbents in sampling and sample preparation steps, and also in chromatography as well as electroanalytical methods.[74,75]

It is well known that the adsorption capacity increases with increasing surface area. This aspect has made MOFs ideal candidates for use in the adsorption process. Literature data indicate that the surface area of MOFs could range from 1000 to up to 14 600 $m^2 g^{-1}$ (envisioned value), which is a significantly greater surface area compared to traditional porous materials such as carbon and zeolites.[76] In 2018, Kaskel and colleagues developed a new porous MOF known as DUT-60, which was formed by Zn_4O^{6+} clusters and an expanded tritopic ligand, 1,3,5-tris(4′-carboxy[1,1′-biphenyl]-4-yl)-benzene, in combination with a ditopic linker, 1,4-bis-*p*-carboxyphenylbuta-1,3-diene. This MOF has a specific surface area of up to ~7800 $m^2 g^{-1}$ and a pore volume of 5.02 $cm^3 g^{-1}$, which is the highest surface area to date.[77] The use of a material with a high specific surface area enables the reduction of the weight of the sorbent used in relation to other materials with a smaller specific surface area while maintaining satisfactory adsorption efficiency.[78] The reduction of the sorbent mass allows for the reduction of the amount of solvents used and the analysis time, which is very beneficial from the GAC standpoint. Another property that increases the environmental friendliness of MOFs as adsorbents is the possibility of their regeneration and reuse. Depending on the type of material used, the application, and the method of regeneration, it is possible to use sorbents a few or even several dozen times,

without significant loss in their adsorption capacity.[79,80] Regeneration of sorbents allows for the reduction of both cost and energy.

1.4.1 Toxicity Issues of MOFs

Despite such advantageous properties, it should be kept in mind that MOFs also have some limitations. Due to their low thermal, chemical, and water stability, some MOFs cannot be used in analytical instrumentation. For example, those with low thermal stability cannot be used as stationary phases in GC, nor can those with low moisture stability be used in aqueous sample analysis.[75,81] However, intensive work is underway to improve these properties and increase their scope of application in this field.

Due to the great properties of MOFs, their application is increasing every year. However, it also raises concerns about their impact on the environment and health. During the production, application, and disposal of MOF materials, they can be released into the environment.[82] It is therefore crucial to determine the concentration of these compounds in various components of the environment as well as to assess the short- and long-term effects of such exposure. An assessment of their environmental safety is particularly important because, given their structure and physicochemical properties, they can be potentially toxic.

Most MOFs are thermally and chemically stable (some MOFs even up to 500 °C), so they can accumulate in the body, while in the case of less stable forms, metal might be released from the MOF and enter the environment.[83] Cd^{2+}, Fe^{2+}, Fe^{3+}, Ni^{2+}, Zn^{2+}, Co^{2+}, and Cu^{2+} are the most commonly used metals in the synthesis of MOFs. In general, most of them are considered to be the least toxic, while cadmium is among the most toxic heavy metals, even at very low concentrations.[84] Hence, such exposure can have very negative effects. Moreover, the downsizing of materials to the nanoscale can significantly contribute to the harmfulness of MOFs. It has been proven that the smaller the particle size, the greater the reactivity, which is directly related to their translocation and toxicity.[85,86]

Unfortunately, toxicological data on MOF materials are still rarely reported in the literature. As a result, the mechanism and origin of MOF toxicity remain largely unknown. To date, several studies have been conducted to determine the toxicity of these materials to different organisms, *e.g.*, bacteria, algae, plants, different cell lines, and animals.[71,82,87–89] For instance, the toxicity and mild photosynthetic inhibitory properties of a copper-based MOF (MOF-199) to pea plants (*Pisum sativum* L.) were observed at 100 and 1000 $mg\,L^{-1}$.[82] In another study, meanwhile, MOF-199 was found to be nontoxic to bacteria (*Escherichia coli* and *Staphylococcus aureus*) at low concentrations, where complete inhibition of bacterial growth was observed after exposure to concentrations $\geq$900 $mg\,L^{-1}$.[90] In the case of studies on the toxicity of aluminium-based porphyrin MOFs to microalgae, both a reduction in the chlorophyll content and an inhibition of algal growth were also reported.[71] In studies using higher organisms, no toxic effects were

found in rats after intravenous administration of very high doses (up to 220 mg kg^{-1}) of three different MOFs of iron carboxylates.[88] Another study revealed that, unlike the submicron-scale cobalt-based zeolitic imidazolate framework (ZIF-6), the nanoscale form interfered with the function of the neuropeptide signalling pathway and impaired learning and memory in rats.[91] MIL-100(Fe) (at concentrations up to 160 g mL^{-1}) was also shown to have a negative effect on normal human liver cell membranes. Aptamer-templated silver nanoclusters embedded in a zirconium MOF, on the other hand, showed low cytotoxicity to MCF-7 cells at concentrations ranging from 5 to 50 g mL^{-1}.[92] In contrast, an Fe-based MOF, MIL-53(Fe), employed as a carrier for an anticancer drug, was found to be nontoxic to HepG2 cells.[93]

The lack of comprehensive toxicological data as well as large discrepancies in the reported ones and the rapid development of MOFs pose more challenges for biosafety assessment. Especially the large variety of metal clusters and organic ligands, as well as the possibility of functional surface modification and significant differences in particle size, makes it very difficult to predict their toxicity. Therefore, more comprehensive and wide-ranging research is needed to determine all the environmental and health effects associated with the use of MOFs.

1.5 MOFs as Green Media in Analytical Chemistry

Traditional extraction methods are labour-intensive and consume large amounts of toxic chlorinated organic solvent and need a large volume of sample.[94] To overcome these disadvantages, miniaturized protocols and solventless techniques were introduced mainly in the late 1990s. Obviously, to achieve the same analytical performance as traditional materials in traditional methods, miniaturized techniques require materials which can perform extraction or separation very efficiently. That's because in a miniaturized system, the amount of extracting phase (or stationary phase in the case of chromatography) is very small. As a result, any phase which is desired to be used in a miniaturized system should have a very high surface area, which means that it needs to be highly porous. The use of MOFs as novel sorbent materials in various aspects of analytical chemistry, especially in sample preparation methods, and as stationary phases in chromatography is directly related to the GAC approach. As mentioned previously, MOFs are classified as extremely ordered crystalline metal clusters with high porosity (>90%) and extremely large specific surface area (up to 7410 $m^2 g^{-1}$), composed of metal oxide clusters and organic linkers.[65,95,96] The metal ions act as nodes or centres and the organic linkers act as bridges between them, forming complex two- or three-dimensional networks. These nodes and ligands are termed secondary building units (SBUs). The variation of metal oxides and the appropriate choice of organic linkers allow the pore size, volume, and functionality to be tailored for designable applications. Also, the characteristics of MOFs mainly depend on the nature of the selected inorganic and organic nodes and ligands and their connectivity. The design

of a MOF implies smart selection of SBUs. Clearly, possible metal–linker combinations are countless. In fact, the Cambridge Crystallographic Data Center contains more than 75 000 different registered MOF structures.[78] While some scientists consider all MOFs as green adsorbents/catalysts, because they are recyclable, we believe for a MOF to be categorized as ''green'', it must have one or both of these features: it must contain biocompatible materials in its structure and/or be synthesized through a green procedure. Moreover, it may be important to understand what products are released from its degradation when a MOF enters into the environment. A good example of application of a green MOF in analytical chemistry is a solid-phase microextraction (SPME) fibre coating fabricated based on the MOF CIM-80(Al),[97] which has both the mentioned green aspects. The CIM-80(Al) MOF was prepared in an aqueous medium and characterized by low cytotoxicity, while a nitinol support was used a biocompatible material. Ethanol was the sole solvent used in the entire fabrication process of the fibre and also for cleaning the coating. Besides, SPME methods are completely solvent-free and are operated in a single step. Recently, a new subclass of MOFs combining supramolecular chemistry and bioscience has emerged, so-called biological metal–organic frameworks (bio-MOFs). Bio-MOFs are composed of biocompatible transition metal ions (*e.g.*, Zn and Fe) coordinated by rigid or flexible biomolecules with functional groups which can be selected to be highly specific towards analytes of interest. Bio-MOFs have the advantages of environmentally friendly designs, low toxicity, biocompatibility, and intrinsic capability to drive molecular recognition processes.[98,99]

In the following subsections, applications of such green MOFs are explained in three parts: their applications in sensors, as green sorbents in extraction processes, and as chromatographic stationary phases. It should be noted that in some cases a MOF may act just as a solid support for a green coating such as a deep eutectic solvent (DES).

1.5.1 MOFs as Green Sorbents in Sensors

This section presents some recent progress in the application of MOFs in the sensing field. A sensor can be regarded as a material or device which measures a physical or chemical quantity and converts it into an electrical signal for detection of specific species in a sample at trace levels.[100] Commercial sensors work based on organic–polymeric or inorganic–semiconductor films that adsorb or react with analyte molecules. This interaction results in changes in electrical or mechanical properties of these films, which can then be monitored. For example, a hydrogen gas sensor works based on the reversible adsorption of H_2 using a film made of spongy palladium. Analytical methods that function based on sensors have some unique advantages such as simple operation, small size, fast response, and being economical. They are also appropriate for large-scale sample screening. As a result of these advantages, sensors have found wide application in medical, environmental, and industrial monitoring; however, at present,

sensors suffer from some disadvantages like low sensitivity, non-specificity, low lifetimes, and mechanical instability. Some chemi-resistive sensors, based on metal oxides, only operate at temperatures above 200 °C, because they need to promote reaction of surface-bound oxygen species.[101] To overcome these limitations, many advanced materials have been developed to construct various robust sensors. Among them, MOFs are especially attractive as novel sensing materials. Again, the large specific surface area of MOFs improves sensor sensitivity. Moreover, the interaction force and the structural matching between the analyte and MOF receptors can be manipulated to have better reversibility and response time to the analyte, leading to the regeneration and real-time monitoring of the compound of interest.[102] In order to develop a green MOF sensor, its design should not only have the two properties mentioned earlier, but it must also have appropriate signal transduction capabilities, and integration of MOFs into devices by employing thin-film growth techniques should be possible as well. Sensors based on MOF photoluminescence are the most common, and because the linkers in their MOFs contain aromatic subunits to be able to illuminate with blue light, it is not surprising that a very large number of optical MOF sensors cannot be regarded as green. MOFs and their derived materials have recently drawn wide attention in electroanalytical chemistry for preparation of electrochemical sensors, which can be categorized into amperometric, impedance, electrochemiluminescence, and photoelectrochemical sensors. Of them, ZIFs are examples in which zeolites and other materials are used and can be regarded as green. As an example, in 2009, the ZIF-8 MOF was employed to synthesize Co_3O_4 NPs,[103] and Kleist *et al.* found that the template-based method can control the size of the NPs to improve its electrocatalytic activity. Therefore, they fabricated an amperometric sensor for glucose using these NPs. At present, most sensors based on MOFs and their derived materials cannot be regarded as green because of the presence of aromatic rings in their structure. Interferences and other restrictions of using these MOF-based sensors can be found in a comprehensive review paper published recently.[100]

1.5.2 MOFs as Green Sorbents in Extraction Processes

While many companies in the world which are involved in sample preparation offer a wide range of commercial materials as sorbents, recent revolution in chemical analysis due to miniaturization has made the need for more selective materials and the requirement of higher capacity for analyte adsorption in complicated matrices more pressing. As a result, the development of robust and highly efficient sorbents, greener if possible, for SPE is indispensable.[104] Therefore, recent trends focus their efforts on the development of MOFs and similar materials as novel extractants to satisfy modern analytical applications. It should be emphasized again that their high porosity and huge surface area make MOFs very interesting adsorbents. Besides, they have outstanding properties such as tunability and the possibility of

designing highly specific materials by reticular chemistry. On the other hand, despite the clear advantages of SPE, it is still far from a green technique, because of the consumption of organic solvents. Miniaturized versions of SPE (mSPE) imply the use of sorbent amounts between 2 and 500 mg, which not only reduces the amount of required sample for analysis, but also ensures less consumption of organic solvents during elution. This greener mSPE mode is particularly useful in dispersive mode because it allows an efficient transfer of analytes to the sorbent material in a short time during microextraction. The dispersion of the sorbent can be performed by ultrasound, simple stirring, vortex, and so on. Sometimes simple devices containing sorbents can be used; in these devices, the sorbent can be properly dispersed into the sample solution to attain high sample–sorbent contact. For example, a pipette tip micro-solid-phase extraction (PT-μSPE) setup is used in which a few mg of (MOF) sorbent is placed between two filters, and as the sample solution passes through it, the sorbent is dispersed in it. Another simple device involves application of a magnet when incorporating magnetic materials as sorbents, in the so-called magnetic (and dispersive) based mSPE mode. In this approach, the magnetic material containing the extracted analytes can be separated from the sample by application of an external magnetic field. While improvements in dispersive mSPE strategies are in progress, the search for novel materials is also in progress, not only for enhancement of sample preparation techniques, but also for achieving green analytical goals. These novel sorbents should have acceptable chemical and mechanical stability under extraction conditions, be reusable, have the ability to interact with analytes through different mechanisms such as absorption and adsorption, have fast kinetics, have high dispersion capacity in liquid samples, and have large specific surface area. In recent decades, many efforts have been made for the preparation and development of selective and robust new coating materials as extraction media for these techniques, including mesoporous silica, carbon nanomaterials, metal and metal oxide NPs, molecularly-imprinted polymers,[105] sputtered silicone,[106] and, more recently, MOFs.[107] Among them, MOFs seem to have all of these characteristics. Moreover, MOFs are characterized by their easy synthesis.[108] These features make MOFs excellent candidates for both SPE and as chromatographic stationary phases, where a highly selective medium with high surface area and solvent and thermal stability under harsh conditions (*e.g.*, extreme pHs) is required. They have uniform structured nanoscale cavities, uniform pore topologies, and high adsorption affinity. Moreover, their structure can be easily tuned for specific applications. For extraction processes, MOFs can be utilized in various modes of SPE such as SPE itself as an exhaustive extraction technique, or miniaturized modes of SPE such as SPME, SBSE, and μSPE (including batch, dispersive, spin-column, PT-μSPE, and microcolumn[100]) (Figure 1.13). To obtain robust MOF-based coatings on SPME or SBSE fibres, adhesion of the coating to the fibre surface is required. For SPME, normally metallic fibres are etched with acids and then they are immersed in MOF precursor solution under suitable

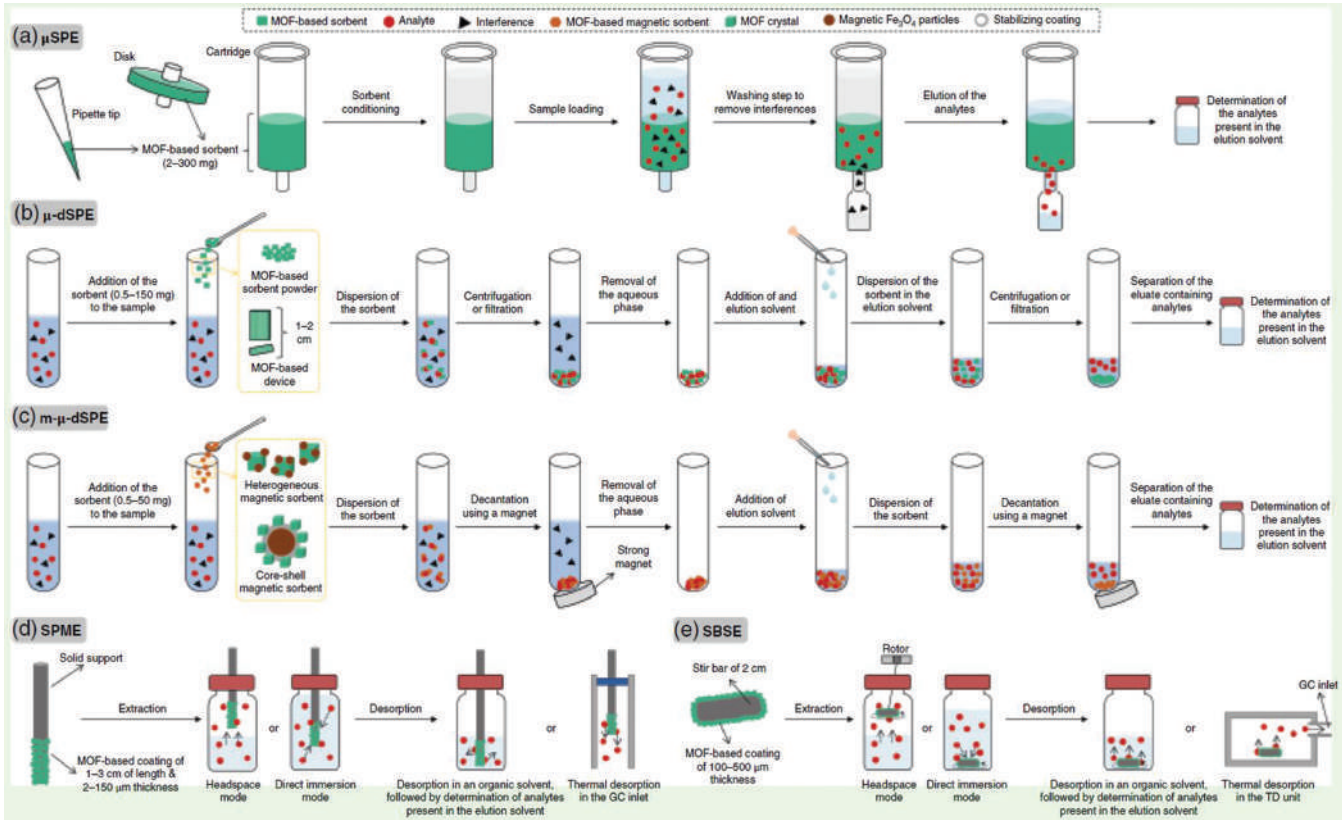

Figure 1.13 Summary of solid-based microextraction methods using MOF-based materials as extraction sorbents: (a) μ-SPE: miniaturized solid-phase extraction; (b) μ-dSPE: micro-dispersive solid-phase extraction; (c) m-μ-dSPE: magnetically assisted micro-dispersive solid-phase extraction; (d) SPME: solid-phase microextraction. SBSE: stir-bar sorptive extraction, GC: gas chromatography, TD: thermal desorption. Reproduced from ref. 101 with permission from John Wiley & Sons, Copyright 2004.

temperature, time, and pressure conditions. As can be seen, this protocol can be regarded as an environmentally friendly procedure since no harmful reagents are utilized during preparation. However, due to the weak binding between the fibre and MOF coating, it is restricted to headspace SPME analysis. To date, MOF-based fibres in direct immersion SPME applications show low reusability unless they are included in non-green complex composites, with the MOF not being the unique sorbent material of the coating. One alternative green method is using chemical vapour deposition of MOFs on both fibres and stir bars. Chemical vapour deposition has already been utilized in one of our previous studies,[109] resulting in thin, homogeneous, crystalline, and porous coatings. No solvents are needed for preparation of these extracting SBSE and SPME fibres; however, due to the cylindrical shape of the supports, it is hard to deposit a uniform coating on them, which has a drawback mainly in terms of the repeatability of the method. The chemical vapour deposition method has been demonstrated for the deposition of different MOFs, such as ZIF-8 and ZIF-67, isoreticular microporous 3D-MOFs based on Zn(II) or Co(II) ions connected with 2-methylimidazolate linkers.[110] Full information about recent progress in application of MOF-derived materials to sample pretreatment can be accessed through ref. 111.

1.5.3 MOFs as Green Media in Chromatography

Trace analysis of analytes in complicated matrices needs not only appropriate sample preparation techniques, but also powerful separation methods. On the other hand, all chromatographic techniques, which are the most important separation techniques, need a stationary phase (SP). The SP has great significance to the power of separation, and so has been under development continuously. MOFs as an important class of hybrid porous materials have received considerable attention in this regard, because of their high selectivity due to the combination of molecular sieving and adsorption effects. While many attempts were made in recent years to apply MOFs as stationary phases for chromatography,[112,113] it is proved that direct application of MOFs in liquid chromatography columns does not have enough efficiency due to the inhomogeneous packing of crystals with irregular shapes. Another limitation in using MOFs is the high back pressure required for the mobile phase to flow through these adsorbents; therefore, special MOFs in the presence of silica particles were synthesized, with silica as a core and MOF crystals as a shell for it.[114] The aforementioned limitation is less serious in applications of MOFs in gas chromatography as stationary phases in both packed and coated capillary columns, but the number of MOF materials explored in these applications is limited. As a result of the limited use of MOFs for chromatographic and electrophoretic applications, it is hard to talk about ''green'' MOFs available in this regard. One good example is MIL-53(Al), which is a widely studied MOF for HPLC.[115] It exhibits a nanoporous flexible framework constructed with infinite chains of corner-sharing $AlO_4(OH)_2$ octahedra, connected with 4 BDC linkers,

resulting in 85 nm large 1D rhombic-shaped pores. MIL-53(Al) was synthesized using recycled waste PET bottles according to the principles of green chemistry and applied for HPLC separation.[116] Particles with sizes from 5 to 10 μm were obtained and packed into the columns (100 and 150 mm×4.6 mm i.d.). For all the investigated mixtures the authors reported the optimum conditions and evaluation parameters for separation in detail. For example, a mixture of seven alkyl benzenes was baseline separated on a 100 mm×4.6 mm i.d. column packed with the obtained material. It was calculated that the column had more than 62 000 plates per meter. The green-synthesized MIL-53 was also used for separation of a mixture of acetone, acetophenone, and butyrophenone. In this case, 14.3k plates per m was obtained. The column itself showed a good equilibrium between runtime and resolution as well as low peak tailing. Table 1.5 shows the most significant applications of MOFs in chromatography.[112]

1.5.4 MOFs in Electrophoretic Separations

In 1937, a method for electrophoresis on moving boundaries was developed, and after about 30 years, a capillary electrophoresis (CE) method using 3 mm rotating capillaries was presented. In 1981, high-voltage CE separations in 75 m capillaries were demonstrated for the first time. In the subsequent years, this powerful analytical technique developed significantly not only in terms of instrumentation, but also in terms of methodology and data processing.[117] Nowadays, CE is one of the main separation techniques in which narrow tubular capillaries are used as separation channels for efficient (large and small) molecule separation. Variability in the electrophoretic mobility of solutes provides the basis for separation in electroosmotic flow (EOF) of solution under a high voltage. Due to its high separation efficiency, CE is a technique that is used in many fields; and it is considered to be environmentally friendly compared to other separation techniques due to the consumption of a small amount of organic solvent and the generation of little residues. In addition, CE is well suited to miniaturization due to the simplicity of the instrument design and therefore is still the most common separation technique applied in microfluidic applications.[118]

Nanomaterials have played a very important role in the development of separation techniques in recent years and examples of their use can be seen in many fields which include medicine, biology, and environmental research. Particularly important is their high surface area-to-volume ratio in relation to separation techniques in order to achieve favourable mass transfer.[119] In CE, nanomaterials have the potential to be added to the background electrolyte (BGE) working as pseudo-stationary phases (PSPs) or they can be physically adsorbed or covalently bonded with the capillary wall which results in an additional semi-permanent or permanent internal coating.[119] NPs have been used in capillary and chip-based electrophoresis for better separation performance. The requirements for nanoparticles to be used in CE are shown in Figure 1.14.

Table 1.5 The most significant applications of MOFs in chromatography. Reproduced from ref. 112 with permission from Elsevier, Copyright 2014.

MOF material	Surface area ($g\,cm^{-3}$)	Pore opening (Å)	Pore diameter (Å)	Thermal stability (°C)	Samples	Form
Gas chromatography						
MOF-508, $Zn(BDC)(4,4'\text{-Bipy})_{0.5}$	946	4		360	Alkanes	Packed column
MOF-5, IRMOF-1 ($Zn_4O(BDC)_3$)	630–3046	7.5, 11.2	11, 15	400–480	Xylene isomers & EB	Packed column
					VOCs[b]	Packed column
					Natural gases	Coated capillary
					n-Alkanes	Coated capillary
					POPs[a]	Coated capillary
					VOCs	Packed column
IRMOF-3, ($Zn_4O(NH_2\text{-}BDC)_3$)	1957	9.6		320	POPs	Coated capillary
IRMOF-8, ($Zn_4O(2,6\text{-}NDC)_3$)	1362	12.5	41.8	300	VOCs	Packed column
IRMOF-10, ($Zn_4O(BPDC)_3$)	265	16.7	132.6	300	VOCs	Packed column
HKUST-1, MOF-199, ($Cu_3(BTC)_2$)	404–629	8, 9	12	220–280	Small Lewis-base analytes	Packed column
					Small hydrocarbons	Coated capillary
MIL-47(V), ($V^{IV}O(BDC)$)	800	8.5	8.5	350	Xylene isomers & EB	Packed column
MIL-100(Fe), $([[Fe_3OF_3(BDC)_3]]\cdot nH_2O)$	2040	5.5–8.6	25–29	280	Alkane isomers	Coated capillary
MIL-100(Cr), $([[Cr_3OF_3(BDC)_3]]\cdot nH_2O)$	2153	5.5–8.6	25–29	280	Alkane isomers	Coated capillary
MIL-101(Cr), $(Cr_3O(H_2O)_2F(BDC)_3)$	2736–2907	12, 16	29, 34	300–330	Xylene isomers & EB	Coated capillary
					n-Alkanes	Coated capillary
ZIF-7, (Zn(benzimidazolate)$_2$)		2.9	4.3	480	*n*-Alkanes	Coated capillary
					n-Alkanes	Coated capillary
ZIF-8, Zn(2-methylimidazole)$_2$	1504	3.4	11.4	380–550	Organic vapours and gases	Packed column
					Branched & linear alkanes	Coated capillary
					n-Alkanes	Coated capillary

JUC-110, ([Cd(H-thipc)$_2$]·6H$_2$O)		4.5		≈200	Alcohols from water	Packed column
UiO-66, [Zr$_6$O$_4$(OH)$_4$(BDC)$_6$]		5–7	8–11	480–540	Alkanes & alkylbenzenes	Coated capillary
	614.3		7.5–11		*n*-Hexane & cyclohexane	Packed column
MOF-CJ3 [HZn$_3$(OH)(BTC)$_2$(2H$_2$O)(DMF)]·H$_2$O	525	11.6	11.6	250	Alkanes & aromatic positional isomers	Coated capillary
DMOF-1, [Cu$_2$(BDC)$_2$(DABCO)]	1026–1300				Light hydrocarbons	Coated capillary
High performance liquid chromatography						
MIL-47(V), (V^{IV}O(BDC))	750	8.5	8.5	330–385	Xylene isomers & EB	Packed column
		Pore volume of 0.32 cm^3 g^{-1}				
MIL-101(Cr), (Cr$_3$O(H$_2$O)$_2$F(BDC)$_3$)	2736–2907	12, 16	29, 34	300–330	Substituted aromatics	Packed column
					Fullerenes	Packed column
MIL-53(Al), (Al^{III}(OH)(BDC))	940–1038	8.5	8.5	330–385	Alkylaromatics	Packed column
					Positional isomers	Packed column
		Pore volume of 0.50 cm^3 g^{-1}			Wide range of analytes	Packed column
MIL-100(Fe), ([(Fe$_3$OF$_3$(BDC)$_3$)]·*n*H$_2$O)	1598	5, 9	25, 29	320	Several analytes	Packed column
ZIF-8, Zn(2-methylimidazole)$_2$	1652 alone, 565 with SiO$_2$		5.72, 17.9	280	Endocrine disrupting chemicals and pesticides	Core–shell microspheres packed column ZIF-8@SiO$_2$
		Pore volume of 0.48 cm^3 g^{-1}				
Other chromatographic methods						
MOF-5, IRMOF-1 (Zn$_4$O(BDC)$_3$)		7.5, 11.2	11, 15	400–480	Organic dyes	Single crystal
ZIF-8, Zn(2-methylimidazole)$_2$	1947	3.4	11.6	≈450	Phenolic isomers	PSP[c] for C-EKC[d]
MIL-100(Fe), ([(Fe$_3$OF$_3$(BDC)$_3$)]·*n*H$_2$O)		5, 9	25, 29		Small organic molecules	Coated capillary for CEC[e]
CAU-1, ([Al$_8$(OH)$_4$-(OCH$_3$)$_8$(BDC-NH$_2$)$_6$])	1700 alone, 423 with polymer		4.5, 10		Aromatic carboxylic acids & some model drugs	Composite with P-MA[f] coated capillary for CEC
MIL-101(Cr), (Cr$_3$O(H$_2$O)$_2$F(BDC)$_3$)	2938 alone, 732 with polymer				Various aromatics	Composite with PMA monolithic capillary for CEC & nano-LC

Table 1.5 (*Continued*)

MOF material	Surface area ($g\,cm^{-3}$)	Pore opening (Å)	Pore diameter (Å)	Thermal stability (°C)	Samples	Form
UiO-66, $[Zr_6O_4(OH)_4(BDC)_6]$	881 alone, 321 with polymer				Various aromatics	Composite with PMA monolithic column for HPLC
$Co(D\text{-Cam})_{1/2}(BDC)_{1/2}(tmdpy)$				250	Racemates	Chiral GC separation
$Zn(ISN)_2{\cdot}2H_2O$				350	Racemates	Chiral GC separation
$Ni(D\text{-Cam})(H_2O)_2$				250	Racemates	Chiral GC separation
$[Cu_2(D\text{-Cam})_2(4,4'\text{-bpy})]_n$		19.4, 22.4	5		Racemates	Chiral HPLC separation

[a] Persistent organic pollutants.
[b] Volatile organic compounds.
[c] Pseudo-stationary phase.
[d] Capillary electrokinetic chromatography.
[e] Capillary electrochromatography.
[f] Polymethacrylate.

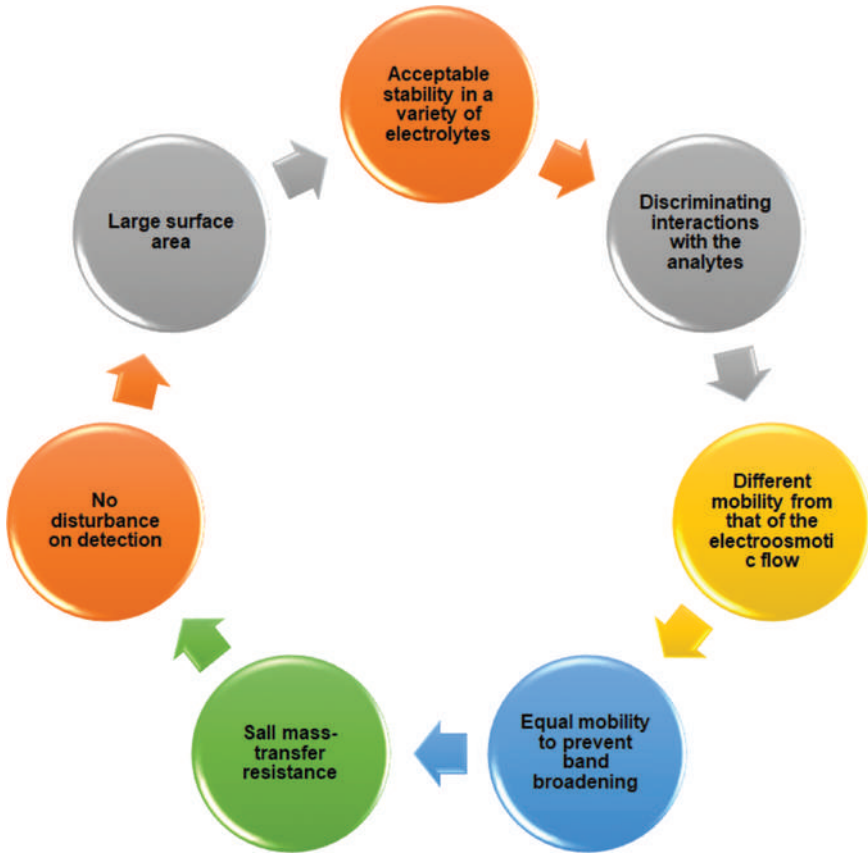

Figure 1.14 Basic requirements for nanoparticles to be used in CE (based on ref. 120).

A number of NPs are used in CE, such as gold nanoparticles (AuNPs), silica nanoparticles (SNPs), carbon nanomaterials, magnetic nanoparticles (MNPs), and MOF nanoparticles (MOF NPs).[121] Currently, MOFs are gaining popularity as a research topic in CE applications.[122] In comparison to carbon nanotubes or graphene, MOFs can be used directly as surfactant-free additives, even under conditions of high ionic strength or in the presence of an electric field.[121] One of the most widely used and well-known MOFs is MIL-101, due to its high mechanical stability and chemical resistibility at pH 0–12 and over a wide range of solvent conditions for two months.[123] An example of the use of the MOF MIL-101 (nMIL-101) as a PSP in CE was its application to the separation of structurally similar anthraquinones. In the experiments conducted, five anthraquinones were separated quickly (8 min) and with high efficiency, with LOD values in the range of 24–57 $\mu g\,L^{-1}$. In addition, the method showed good potential for the analysis of anthraquinones in water samples.[124]

The CE technique is extensively used in the separation of amino acids, and MOFs have also been used in such procedures. An example is the use of ZIF-8 nanocrystals as a stationary phase for CE separation of proteins, which proved to be a cheap, efficient, and environmentally friendly solution. A capillary coated with ZIF-8 nanocrystals, which was characterized by good reproducibility and stability, was successfully used for the separation of D- and L-phenylalanine.[125]

In another study, an attempt was made to synthesize a Mn(cam)(bpy) (where cam: (1*R*,3*S*)-(+)-camphoric acid, bpy: 4,4′-dipyridyl) MOF for use as a stationary phase to modify a capillary column, which was then applied for the determination of ten types of sulphonamides. The open-tube capillary column produced showed good separation capability, stability, and reproducibility.[126]

1.5.5 MOFs as Sensors

Compared to conventional inorganic and organic luminescent sensors, MOF-based sensors have numerous advantages (see Figure 1.15).[127]

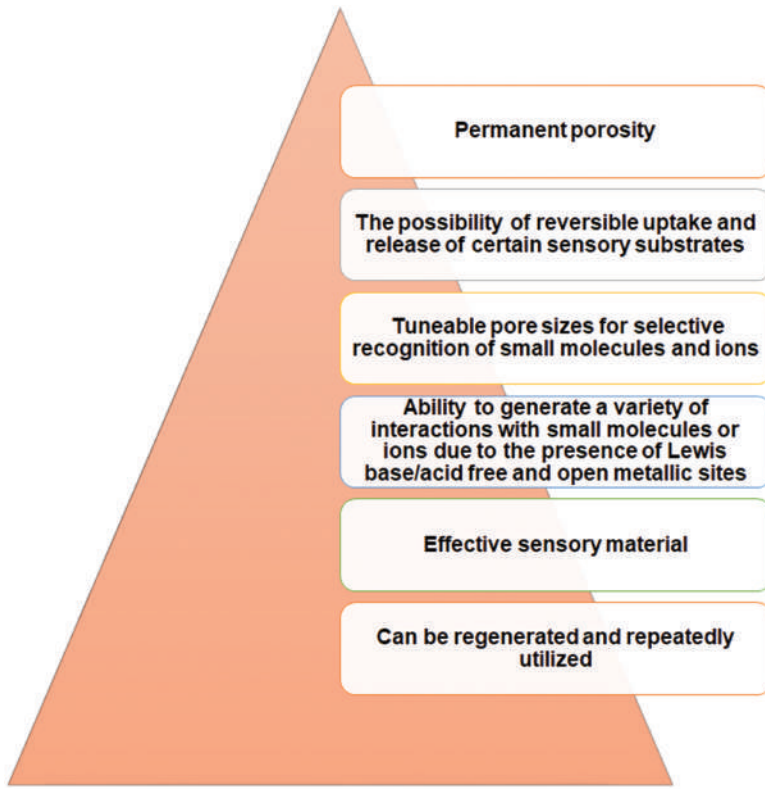

Figure 1.15 Advantages of MOFs used as luminescent sensors.

Luminescent MOFs, most of which are lanthanide-based, have been used to sense cations, anions, small molecules, and explosives.[128] Luminescent MOFs have been also successfully applied for sensing of important targets such as gases and vapours.[129]

MOF-based sensing of Cu^{2+}, Fe^{3+}, Co^{2+}, Ag^{+}, Zn^{2+}, and Mg^{2+} was achieved through the use of interactions, which include:

- metal–ligand coordination interaction (weak binding of the metal to the ligand);
- metal–ligand coordination interaction (weak binding of metal ions to heteroatoms (N or O) in ligands); and
- intramolecular energy transfer from the ligand to metal ion.[130–133]

The sensing of ions such as Ca^{2+}, Cu^{2+}, and Co^{2+}, on the other hand, is based on cation exchange between the target metal ions and non-ramified cations in MOFs.[134,135]

The effect of different cations on the fluorescence spectrum of MOFs has also been extensively described.[133,136] Unusual examples of the use of Ln–Mn, Ln–Fe, and Ln–Ag hetero-MOFs for metal ion recognition and detection were investigated, where a significant increase in fluorescence was observed upon addition of Zn^{2+}, while the introduction of other metal ions such as Mn^{2+}, Ca^{2+}, Mg^{2+}, Fe^{2+}, Co^{2+}, and Ni^{2+} did not change the luminescence intensity but rather decreased it.[137–139] Lanthanide MOFs have also been shown to be highly sensitive and selective in detecting Cu^{2+} in aqueous solution and simulated physiological aqueous solution.[130] In environmental and biological systems many inorganic anions (F^{-}, Cl^{-}, Br^{-}, SO_4^{2-}, *etc.*) play a crucial role; thus the detection of anions using MOFs is also the subject of many interesting studies.[140–142]

Further examples of the use of MOFs are related to the sensing and detection of small molecules. The two-dimensional porous framework $Cu_6L_6{\cdot}(H_2O)$(DMSO) (where HL = 5,6-diphenyl-1,2,4-triazine-3-thiol) was used, which showed highly selective absorption for aromatic molecules in water.[128] Other examples of MOFs are related to recognition and sensing of acetone[142] and nitroaromatic explosives in ethanol solution.[142] However, a family of MOFs with 4,40-oxybis(benzoate) (OBA) ligands and suitable cationic species for recognition of small solvent molecules have been used.[143] Given that many different organic ligands can be assembled into nanoscale MOFs to match their competitive uptake with different analytes, an approach for the detection of small molecules is provided by this strategy that is very promising.

The specific properties of MOFs have also made them useful for sensing gases and vapours. In particular, chemical sensors for the rapid detection of explosives in the gas phase are extremely popular due to their homeland security, environmental monitoring, and humanitarian aid applications. An Yb^{3+}-encapsulating MOF is an example of luminescent MOFs for sensing oxygen.[144] A very interesting example of luminescent

MOFs with fast response time and fast reversible behaviour for the detection of ethanol vapour molecules is ITQMOF-1-Eu with 4,40-(hexafluoroisopropylidene)bis(benzoic acid) as a ligand.[145] For chemical sensors for the rapid detection of explosives, an example of research could be the use of the MOF $Zn_2(bpdc)_2(bpee)$ (where bpdc = 4,40-biphenyldicarboxylate; bpee = 1,2-bipyridylethene) for detection of both DNT and DMNB (2,3-dimethyl-2,3-dinitrobutane) with rapid response and high sensitivity.[146] MOFs can also be used to detect the pH value, temperature, and ionizing radiation.[128]

1.5.5.1 Electroluminescent and Optical Sensors

The luminescence properties of MOFs represent a very interesting area of research for sensing purposes. The luminescence properties of MOFs are very sensitive to and depend on their structural features, the coordination environments of metal ions, and the nature of the pore surface as well as their interactions with guest species *via* coordination and hydrogen bonds, π–π interactions, and electron and energy transfer processes.[127] Luminescent MOFs have so far been used in research on: the fundamental synthesis itself and determination of their luminescent properties; the creation of MOFs with tunable luminescence, which have subsequently been used in light-emitting devices and displays; the application of luminescent MOFs to explore the local environment, structure, and guest species; and the development of multifunctional MOFs combining luminescence, magnetic properties, and biocompatibility essential for biomedical purposes.[128] Luminescent MOFs have also been investigated for their potential applications in fluorescence sensing, nonlinear optics, and photocatalysis.

An example of MOF application can be found in research where a method for luminescence tuning by modifying the concentration of lanthanide ions is discussed.[147] Another example where the luminescence colour can be easily tuned from green to green-yellow, yellow, orange, and red-orange is the use of a terbium 1,3,5-benzenetricarboxylate MOF doped with Eu^{3+} ions.[148] Replacement and modification of guest species may also result in significant changes in the luminescence spectrum of MOFs.[149]

1.5.5.2 Electrochemical Sensors

Due to the insulating nature of the organic ligand and the relatively low stability in aqueous solution, MOFs are regarded as poor electrical conductors. However, thanks to the intensive development of nanoscience, it has been possible to introduce methodological solutions to overcome these limitations. One of the most commonly applied methods is to integrate MOFs with a variety of highly conductive and mechanically durable materials. With flexible porous structures, large surface areas, and various sizes, MOFs have been successfully combined with diverse materials, *e.g.*, carbon materials, noble metal nanoparticles, metal/metallic oxide nanoparticles,

conductive polymers, and quantum dots, thus extending their application for target analysis.[150] According to a literature review, MOF-based electrochemical sensors have been widely applied in various research fields such as medicine, public health, energy control, and environmental pollutant detection to monitor different compounds such as anions, heavy metal ions, organic compounds, and gases, as well as large molecules, proteins, biomarkers, DNA, *etc.*[151,152] Due to their outstanding conductivity, low cost, large specific surface areas, tensile strength, and chemical stability, carbon materials are particularly highly preferred over other species. Activated carbon, carbon nanotubes, carbon nanofibres, graphene, graphene oxide and reduced graphene oxide, graphene nanosheets, and graphene and carbon aerogels and hydrogels have all been successfully used as MOF modifiers.[151,153,154] For example, an Fe-based MOF doped into carbon nanofibres was used for the detection of tetracycline. Upon optimization, this electrochemical sensor exhibited a linear range of 0.1–105 nM tetracycline with an LOD of 0.01 nM.[155] Meanwhile, by integrating UiO-66-NH_2 with a graphene aerogel, the detection of multiple heavy metal ions (Cd^{2+}, Pb^{2+}, Cu^{2+}, and Hg^{2+}) in water, soil, and vegetable samples was possible.[156] Moreover, Ce/UiO-66@MWCNT as a conductive component in an electrochemical biosensor was used for organophosphate pesticide detection.[157] Additionally, by immobilization of porous biomass carbon onto the surfaces of MOFs *via* a hydrothermal reaction process, it was possible to obtain an electrochemical sensor that had wide linear ranges and low LODs for the determination of dopamine, acetaminophen, and xanthine in human serum.[158] In addition to those mentioned, reports on the integration of MOFs with acetylene black, platelet ordered mesoporous carbon,[159] graphene oxide nanoribbons,[160] and carbon nanohorns[161] have also been published. The areas of other modifier groups' applications will be discussed in detail in later chapters.

Despite the tremendous progress achieved in recent years for electrochemical applications of various nanomaterials and MOFs, several issues and challenges remain in this field. However, electroanalytical methods are quite efficient, fast, very simple, and reproducible; thus they are compatible with the concept of GAC. Therefore, it is expected that in the future many researchers from various scientific disciplines will pay close attention to research on MOF electrochemical sensors and their applications.

1.6 Concluding Remarks

MOFs are recognized as green sorbent materials in analytical chemistry due to their unique properties such as the highest known surface areas, mechanical and thermal stability, selectivity, and reusability. As the application of MOFs can easily meet the principles of GAC, analytical chemistry has benefited a lot from the potential of MOF applications. MOFs have proven successful as sorbent materials in extraction/microextraction processes, as sensors, and as stationary or pseudo-stationary phases in chromatographic systems. They can be designed to selectively extract any type of analyte from

aqueous media. However, considering the GAC principles, assurance of MOF sustainability must begin with MOF design, followed by an adequate synthetic methodology and toxicity evaluation of the resulting material, resulting in an analytical methodology that can be categorized as a GAC procedure. Moreover, use of MOFs as adsorbents is faced with challenges: for example, they are expensive and require additional and time-consuming steps such as centrifugation and filtration for their recovery. Techniques such as PT-μSPE and combination of MOFs with magnetic NPs offered higher extraction efficiency and easy magnetic recovery. MOFs hold potential for extraction of micro-organisms. Also, more efforts are necessary to better design low priced MOFs which can be applied on a large scale, for example in preparative applications. It is also of importance to do more research on the long-term toxicity of these materials, especially for their long-term use. Taking all of these into consideration, a significant collaboration between materials science and analytical chemistry, with an emphasis on green chemistry, should be encouraged and strengthened.

References

1. N. Stock and S. Biswas, *Chem. Rev.*, 2012, **112**, 933–969.
2. H. Furukawa, N. Ko, Y. B. Go, N. Aratani, S. B. Choi, E. Choi, A. Ö. Yazaydin, R. Q. Snurr, M. O'Keeffe and J. Kim, *Science*, 2010, **329**, 424–428.
3. O. K. Farha, I. Eryazici, N. C. Jeong, B. G. Hauser, C. E. Wilmer, A. A. Sarjeant, R. Q. Snurr, S. T. Nguyen, A. O. Z. R. Yazaydın and J. T. Hupp, *J. Am. Chem. Soc.*, 2012, **134**, 15016–15021.
4. T.-H. Chen, I. Popov, Y.-C. Chuang, Y.-S. Chen and O. Š. Miljanić, *Chem. Commun.*, 2015, **51**, 6340–6342.
5. B. Zhou, P. Ma, H. Chen and C. Wang, *Chem. Commun.*, 2014, **50**, 14558–14561.
6. O. M. Yaghi, M. O'Keeffe, N. W. Ockwig, H. K. Chae, M. Eddaoudi and J. Kim, *Nature*, 2003, **423**, 705–714.
7. M. Gaab, N. Trukhan, S. Maurer, R. Gummaraju and U. Müller, *Microporous Mesoporous Mater.*, 2012, **157**, 131–136.
8. P. Tundo, P. Anastas, D. S. Black, J. Breen, T. J. Collins, S. Memoli, J. Miyamoto, M. Polyakoff and W. Tumas, *Pure Appl. Chem.*, 2000, **72**, 1207–1228.
9. P. Anastas and N. Eghbali, *Chem. Soc. Rev.*, 2010, **39**, 301–312.
10. M. M. Unterlass, *Eur. J. Inorg. Chem.*, 2016, **2016**, 1135–1156.
11. X. Meng and F.-S. Xiao, *Chem. Rev.*, 2014, **114**, 1521–1543.
12. J. Juillard, *Pure Appl. Chem.*, 1977, **49**, 885–892.
13. A. Pichon, A. Lazuen-Garay and S. L. James, *CrystEngComm*, 2006, **8**, 211–214.
14. T. Friščić, *J. Mater. Chem.*, 2010, **20**, 7599–7605.
15. S. M. McKenna, S. Leimkühler, S. Herter, N. J. Turner and A. J. Carnell, *Green Chem.*, 2015, **17**, 3271–3275.

16. C. Volkringer, D. Popov and T. Loiseau, *Chem. Mater.*, 2009, **21**, 5695–5697.
17. H. Reinsch, *Eur. J. Inorg. Chem.*, 2016, **2016**, 4290–4299.
18. C. Gucuyener, J. van den Bergh, J. Gascon and F. Kapteijn, *J. Am. Chem. Soc.*, 2010, **132**, 17704–17706.
19. S. Gao, Y. Sui, F. Wei, J. Qi, Q. Meng, Y. Ren and Y. He, *Nano*, 2019, **14**, 1950032.
20. S. Bhattacharjee, J.-S. Choi, S.-T. Yang, S. B. Choi, J. Kim and W.-S. Ahn, *J. Nanosci. Nanotechnol.*, 2010, **10**, 135–141.
21. S. D. Bagi, A. S. Myerson and Y. Román-Leshkov, *Cryst. Growth Des.*, 2021, **21**, 6529–6536.
22. A. M. Joaristi, J. Juan-Alcañiz, P. Serra-Crespo, F. Kapteijn and J. Gascon, *Cryst. Growth Des.*, 2012, **12**, 3489–3498.
23. Z. Song, L. Zhang, K. Doyle-Davis, X. Fu, J. L. Luo and X. Sun, *Adv. Energy Mater.*, 2020, **10**, 2001561.
24. W. Kleist, M. Maciejewski and A. Baiker, *Thermochim. Acta*, 2010, **499**, 71–78.
25. G. Sargazi, D. Afzali and A. Mostafavi, *Ultrason. Sonochem.*, 2018, **41**, 234–251.
26. M. Zeraati, M. Moghaddam-Manesh, S. Khodamoradi, S. Hosseinzadegan, A. Golpayegani, N. P. S. Chauhan and G. Sargazi, *J. Mol. Struct.*, 2022, **1247**, 131315.
27. A. Asfaram, M. Ghaedi and M. K. Purkait, *Ultrason. Sonochem.*, 2017, **38**, 463–472.
28. G. Sargazi, D. Afzali, N. Daldosso, H. Kazemian, N. Chauhan, Z. Sadeghian, T. Tajerian, A. Ghafarinazari and M. Mozafari, *Ultrason. Sonochem.*, 2015, **27**, 395–402.
29. W. Sun, X. Zhai and L. Zhao, *Chem. Eng. J.*, 2016, **289**, 59–64.
30. M. Zeraati, V. Alizadeh, S. Chupradit, N. P. S. Chauhan and G. Sargazi, *J. Mol. Struct.*, 2022, **1250**, 131712.
31. N. E. Travia, B. L. Scott and J. L. Kiplinger, *Chem. – Eur. J.*, 2014, **20**, 16846–16852.
32. S. Ashley, R. Fenner, W. Nuttall and G. Parks, *Energy Convers. Manage.*, 2015, **101**, 136–150.
33. H. Abbasi, P. Kazemzadeh, T. Shahryari, M. Zeraati, N. P. S. Chauhan and G. Sargazi, *Appl. Phys. A: Mater. Sci. Process.*, 2022, **128**, 869.
34. S. Kitagawa, *Chem. Soc. Rev.*, 2014, **43**, 5415–5418.
35. G. Sargazi, D. Afzali, A. Mostafavi and S. Y. Ebrahimipour, *J. Solid State Chem.*, 2017, **250**, 32–48.
36. N. D. Burrows, S. Harvey, F. A. Idesis and C. J. Murphy, *Langmuir*, 2017, **33**, 1891–1907.
37. M. Zeraati, A. Mohammadi, S. Vafaei, N. P. S. Chauhan and G. Sargazi, *Front. Chem.*, 2021, **9**, 722990.
38. Z. Branson, T. Dasgupta and D. B. Rubin, *Ann. Appl. Stat.*, 2016, **10**(4), 1958–1976.
39. H. Sun, Q. Yang and J. Hao, *Adv. Colloid Interface Sci.*, 2016, **235**, 14–22.

40. N. Kovalchuk, A. Trybala, O. Arjmandi-Tash and V. Starov, *Adv. Colloid Interface Sci.*, 2016, **233**, 155–160.
41. W. Zhao and Y. Wang, *Adv. Colloid Interface Sci.*, 2017, **239**, 199–212.
42. S. Shafiee, H. A. Ahangar and A. Saffar, *Carbohydr. Polym.*, 2019, **222**, 114982.
43. H. Y. Yen and C. P. Lin, *Desalin. Water Treat.*, 2016, **57**, 11154–11161.
44. K. Pirzadeh, A. A. Ghoreyshi, M. Rahimnejad and M. Mohammadi, *Front. Chem. Sci. Eng.*, 2020, **14**, 233–247.
45. G. Zolfaghari, A. Esmaili-Sari, M. Anbia, H. Younesi, S. Amirmahmoodi and A. Ghafari-Nazari, *J. Hazard. Mater.*, 2011, **192**, 1046–1055.
46. K. Esfandiari, A. R. Mahdavi, A. A. Ghoreyshi and M. Jahanshahi, *Int. J. Hydrogen Energy*, 2018, **43**, 6654–6665.
47. M. S. Phadke, *Quality Engineering Using Robust Design*, PTR Prentice-Hall, Englewood Cliffs, NJ, 1989.
48. P. Khare and A. Kumar, *Appl. Water Sci.*, 2012, **2**, 317–326.
49. Y. Jiang, X. Zhang, X. Dai, W. Zhang, Q. Sheng, H. Zhuo, Y. Xiao and H. Wang, *Nano Res.*, 2017, **10**, 876–889.
50. A. Nikseresht, A. Daniyali, M. Ali-Mohammadi, A. Afzalinia and A. Mirzaie, *Ultrason. Sonochem.*, 2017, **37**, 203–207.
51. N. A. Khan and S. H. Jhung, *Coord. Chem. Rev.*, 2015, **285**, 11–23.
52. M. R. Armstrong, S. Senthilnathan, C. J. Balzer, B. Shan, L. Chen and B. Mu, *Ultrason. Sonochem.*, 2017, **34**, 365–370.
53. P. George, N. R. Dhabarde and P. Chowdhury, *Mater. Lett.*, 2017, **186**, 151–154.
54. G. Sargazi, D. Afzali and A. Mostafavi, *J. Porous Mater.*, 2018, **25**, 1723–1741.
55. H. Fazelirad, M. Ranjbar, M. A. Taher and G. Sargazi, *J. Ind. Eng. Chem.*, 2015, **21**, 889–892.
56. H. Reinsch and N. Stock, *Dalton Trans.*, 2017, **46**, 8339–8349.
57. P. A. Julien, C. Mottillo and T. Friščić, *Green Chem.*, 2017, **19**, 2729–2747.
58. M. Taddei, *Coord. Chem. Rev.*, 2017, **343**, 1–24.
59. A. W. Thornton, R. Babarao, A. Jain, F. Trousselet and F.-X. Coudert, *Dalton Trans.*, 2016, **45**, 4352–4359.
60. B. S. Gelfand and G. K. Shimizu, *Dalton Trans.*, 2016, **45**, 3668–3678.
61. Y. H. Shih, Y. C. Kuo, S. Lirio, K. Y. Wang, C. H. Lin and H. Y. Huang, *Chem. – Eur. J.*, 2017, **23**, 42–46.
62. M. Sánchez-Sánchez, N. Getachew, K. Díaz, M. Díaz-García, Y. Chebude and I. Díaz, *Green Chem.*, 2015, **17**, 1500–1509.
63. C. Avci-Camur, J. Troyano, J. Pérez-Carvajal, A. Legrand, D. Farrusseng, I. Imaz and D. Maspoch, *Green Chem.*, 2018, **20**, 873–878.
64. P. A. Bayliss, I. A. Ibarra, E. Pérez, S. Yang, C. C. Tang, M. Poliakoff and M. Schröder, *Green Chem.*, 2014, **16**, 3796–3802.
65. M. Zeraati, A. Rahdar, D. I. Medina and G. Sargazi, *Front. Chem.*, 2021, 1054.
66. S. Zhang, F. Rong, C. Guo, F. Duan, L. He, M. Wang, Z. Zhang, M. Kang and M. Du, *Coord. Chem. Rev.*, 2021, **439**, 213948.

67. X. Zhang, X. Sun, T. Lv, L. Weng, M. Chi, J. Shi and S. Zhang, *J. Mater. Sci.: Mater. Electron.*, 2020, **31**, 13344–13351.
68. D. Wang, H. Wu, W. Q. Lim, S. Z. F. Phua, P. Xu, Q. Chen, Z. Guo and Y. Zhao, *Adv. Mater.*, 2019, **31**, 1901893.
69. H. Zhang, S. Hwang, M. Wang, Z. Feng, S. Karakalos, L. Luo, Z. Qiao, X. Xie, C. Wang and D. Su, *J. Am. Chem. Soc.*, 2017, **139**, 14143–14149.
70. A. E. Fazary, H. A. Ibrahium, M. A. Youssef, N. S. Awwad and H. S. Abd-Rabboh, *J. Solution Chem.*, 2019, **48**, 1716–1729.
71. Y. Li, S. Shang, J. Shang and W.-X. Wang, *Environ. Pollut.*, 2021, **291**, 118199.
72. M. Safaei, M. M. Foroughi, N. Ebrahimpoor, S. Jahani, A. Omidi and M. Khatami, *TrAC, Trends Anal. Chem.*, 2019, **118**, 401–425.
73. B. Hashemi, P. Zohrabi, N. Raza and K.-H. Kim, *TrAC, Trends Anal. Chem.*, 2017, **97**, 65–82.
74. P. Rocío-Bautista, I. Taima-Mancera, J. Pasán and V. Pino, *Separations*, 2019, **6**, 33.
75. M. Bazargan, F. Ghaemi, A. Amiri and M. Mirzaei, *Coord. Chem. Rev.*, 2021, **445**, 214107.
76. P. Sharanyakanth and M. Radhakrishnan, *Trends Food Sci. Technol.*, 2020, **104**, 102–116.
77. I. U. Din, M. Usman, S. Khan, A. Helal, M. A. Alotaibi, A. I. Alharthi and G. Centi, *J. CO_2 Util.*, 2021, **43**, 101361.
78. A. Gutiérrez-Serpa, I. Pacheco-Fernández, J. Pasán and V. Pino, *Separations*, 2019, **6**, 47.
79. Z. Pirmohammadi, A. Bahrami, D. Nematollahi, S. Alizadeh, F. Ghorbani Shahna and R. Rahimpoor, *Biomed. Chromatogr.*, 2020, **34**, e4725.
80. Z.-J. Lin, H.-Q. Zheng, H.-Y. Zheng, L.-P. Lin, Q. Xin and R. Cao, *Inorg. Chem.*, 2017, **56**, 14178–14188.
81. X. Lan, H. Zhang, P. Bai and X. Guo, *Microporous Mesoporous Mater.*, 2016, **231**, 40–46.
82. X. Guan, Q. Li, T. Maimaiti, S. Lan, P. Ouyang, B. Ouyang, X. Wu and S.-T. Yang, *J. Hazard. Mater.*, 2021, **409**, 124521.
83. M. Sajid, *Environ. Sci. Pollut. Res.*, 2016, **23**, 14805–14807.
84. M. T. Hayat, M. Nauman, N. Nazir, S. Ali and N. Bangash, in *Cadmium Toxicity and Tolerance in Plants*, Elsevier, 2019, pp. 163–183.
85. M. D. Scherer, J. C. Sposito, W. F. Falco, A. B. Grisolia, L. H. Andrade, S. M. Lima, G. Machado, V. A. Nascimento, D. A. Gonçalves and H. Wender, *Sci. Total Environ.*, 2019, **660**, 459–467.
86. S. Singh, *Toxicol. Mech. Methods*, 2019, **29**, 300–311.
87. C.-H. Lin, C.-M. Li, C.-H. Chen and W.-H. Chen, *Environ. Sci. Pollut. Res.*, 2019, **26**, 20701–20711.
88. T. Baati, L. Njim, F. Neffati, A. Kerkeni, M. Bouttemi, R. Gref, M. F. Najjar, A. Zakhama, P. Couvreur and C. Serre, *Chem. Sci.*, 2013, **4**, 1597–1607.
89. F. Ren, B. Yang, J. Cai, Y. Jiang, J. Xu and S. Wang, *J. Hazard. Mater.*, 2014, **271**, 283–291.

90. B. Ouyang, P. Ouyang, M. Shi, T. Maimaiti, Q. Li, S. Lan, J. Luo, X. Wu and S.-T. Yang, *J. Hazard. Mater. Adv.*, 2021, **1**, 100002.
91. S. Deng, X. Yan, P. Xiong, G. Li, T. Ku, N. Liu, C. Liao and G. Jiang, *Sci. Total Environ.*, 2021, **771**, 145063.
92. F. Su, Q. Jia, Z. Li, M. Wang, L. He, D. Peng, Y. Song, Z. Zhang and S. Fang, *Microporous Mesoporous Mater.*, 2019, **275**, 152–162.
93. X. Leng, X. Dong, W. Wang, N. Sai, C. Yang, L. You, H. Huang, X. Yin and J. Ni, *Molecules*, 2018, **23**, 2490.
94. M. Sargazi, S. H. Hashemi and M. Kaykhaii, *Sample Preparation Techniques for Chemical Analysis*, 2021, p. 9.
95. A. Peristyy, P. N. Nesterenko, A. Das, D. M. D'Alessandro, E. F. Hilder and R. D. Arrua, *Chem. Commun.*, 2016, **52**, 5301–5304.
96. M. Safinejad, A. Rigi, M. Zeraati, Z. Heidary, S. Jahani, N. P. S. Chauhan and G. Sargazi, *BMC Chem.*, 2022, **16**, 1–9.
97. I. Pacheco-Fernández, M. Rentero, J. H. Ayala, J. Pasán and V. Pino, *Anal. Chim. Acta*, 2020, **1133**, 137–149.
98. F. Zhang, X. Zou, X. Gao, S. Fan, F. Sun, H. Ren and G. Zhu, *Adv. Funct. Mater.*, 2012, **22**, 3583–3590.
99. V. Nejadshafiee, H. Naeimi, B. Goliaei, B. Bigdeli, A. Sadighi, S. Dehghani, A. Lotfabadi, M. Hosseini, M. S. Nezamtaheri and M. Amanlou, *Mater. Sci. Eng. C*, 2019, **99**, 805–815.
100. F. S. Mostafavi and D. Zaeim, *Int. J. Biol. Macromol.*, 2020, **159**, 1165–1176.
101. S. Capone, A. Forleo, L. Francioso, R. Rella, P. Siciliano, J. Spadavecchia, D. S. Presicce and A. M. Taurino, *ChemInform*, 2004, **35**, 29.
102. L. E. Kreno, K. Leong, O. K. Farha, M. Allendorf, R. P. Van Duyne and J. T. Hupp, *Chem. Rev.*, 2012, **112**, 1105–1125.
103. W. Kleist, F. Jutz, M. Maciejewski and A. Baiker, *Eur. J. Inorg. Chem.*, 2009, **2009**, 3552–3561.
104. M. Kaykhaii, *'Evolution of Sample Preparation' in Sample Preparation Techniques for Chemical Analysis*, IntechOpen, London, United Kingdom, 2021.
105. S. H. Hashemi, M. Kaykhaii and M. Khajeh, *Anal. Lett.*, 2015, **48**, 1815–1829.
106. A. Diwan, B. Singh, T. Roychowdhury, D. D. Yan, L. Tedone, P. N. Nesterenko, B. Paull, E. T. Sevy, R. A. Shellie, M. Kaykhaii and M. R. Linford, *Anal. Chem.*, 2016, **88**, 1593–1600.
107. P. Rocío-Bautista, A. Gutiérrez-Serpa, A. J. Cruz, R. Ameloot, J. H. Ayala, A. M. Afonso, J. Pasán, S. Rodríguez-Hermida and V. Pino, *Talanta*, 2020, **215**, 120910.
108. Z. S. Moghaddam, M. Kaykhaii, M. Khajeh and A. R. Oveisi, *Spectrochim. Acta, Part A*, 2018, **194**, 76–82.
109. T. Roychowdhury, D. I. Patel, D. Shah, A. Diwan, M. Kaykhaii, J. S. Herrington, D. S. Bell and M. R. Linford, *J. Chromatogr. A*, 2020, **1623**, 461065.
110. I. Stassen, D. De Vos and R. Ameloot, *Chem. – Eur. J.*, 2016, **22**, 14452–14460.
111. Z. Wenmin, L. Qingqing, F. Min, G. Jia, C. Zongbao and Z. Lan, *Chin. J. Chromatogr.*, 2021, **39**, 941–949.
112. K. Yusuf, A. Aqel and Z. ALOthman, *J. Chromatogr. A*, 2014, **1348**, 1–16.

113. A. A. Kotova, D. Thiebaut, J. Vial, A. Tissot and C. Serre, *Coord. Chem. Rev.*, 2022, **455**, 214364.
114. R. D. Arrua, A. Peristyy, P. N. Nesterenko, A. Das, D. M. D'Alessandro and E. F. Hilder, *Analyst*, 2017, **142**, 517–524.
115. C.-X. Yang, S.-S. Liu, H.-F. Wang, S.-W. Wang and X.-P. Yan, *Analyst*, 2012, **137**, 133.
116. A. Aqel, N. Alkatheri, A. Ghfar, A. M. Alsubhi, Z. A. ALOthman and A. Y. Badjah-Hadj-Ahmed, *J. Chromatogr. A*, 2021, **1638**, 461857.
117. V. Adam and M. Vaculovicova, *Electrophoresis*, 2017, **38**, 2389–2404.
118. E. Ban, Y. S. Yoo and E. J. Song, *Talanta*, 2015, **141**, 15–20.
119. M. Á. González-Curbelo, D. A. Varela-Martínez, B. Socas-Rodríguez and J. Hernández-Borges, *Electrophoresis*, 2017, **38**, 2431–2446.
120. Z. Zhang, B. Yan, Y. Liao and H. Liu, *Anal. Bioanal. Chem.*, 2008, **391**, 925–927.
121. S. A. Kitte, T. H. Fereja, M. I. Halawa, B. Lou, H. Li and G. Xu, *Electrophoresis*, 2019, **40**, 2050–2057.
122. P. Kumar, A. Pournara, K. H. Kim, V. Bansal, S. Rapti and M. J. Manos, *Prog. Mater. Sci.*, 2017, **86**, 25–74.
123. K. Leus, T. Bogaerts, J. De Decker, H. Depauw, K. Hendrickx, H. Vrielinck, V. Van Speybroeck and P. Van Der Voort, *Microporous Mesoporous Mater.*, 2016, **226**, 110–116.
124. Y. Liu, J. Hu, Y. Li, Y.-T. Shang, J.-Q. Wang, Y. Zhang and Z.-L. Wang, *Electrophoresis*, 2017, **38**, 2521–2529.
125. Z. Geng, Q. Song, B. Yu and H. Cong, *Talanta*, 2018, **188**, 493–498.
126. X. Wang, N. Ye, X. Hu, Q. Liu, J. Li, L. Peng and X. Ma, *Electrophoresis*, 2018, **39**, 2236–2245.
127. P. Mahata, S. K. Mondal, D. K. Singha and P. Majee, *Dalton Trans.*, 2017, **46**, 301–328.
128. Y. Cui, Y. Yue, G. Qian and B. Chen, *Chem. Rev.*, 2012, **112**, 1126–1162.
129. S. L. Cai, S. R. Zheng, J. Fan, T. T. Xiao, J. B. Tan and W. G. Zhang, *Inorg. Chem. Commun.*, 2011, **14**, 937–939.
130. Y. Xiao, Y. Cui, Q. Zheng, S. Xiang, G. Qian and B. Chen, *Chem. Commun.*, 2010, **46**, 5503–5505.
131. Q. Wang and C. Tan, *Anal. Chim. Acta*, 2011, **708**, 111–115.
132. B. Chen, L. Wang, Y. Xiao, F. R. Fronczek, M. Xue, Y. Cui and G. Qian, *Angew. Chem.*, 2009, **121**, 508–511.
133. W. Liu, T. Jiao, Y. Li, Q. Liu, M. Tan, H. Wang and L. Wang, *J. Am. Chem. Soc.*, 2004, **126**, 2280–2281.
134. W. G. Lu, L. Jiang, X. L. Feng and T. B. Lu, *Inorg. Chem.*, 2009, **48**, 6997–6999.
135. F. Luo and S. R. Batten, *Dalton Trans.*, 2010, **39**, 4485–4488.
136. B. Chen, L. Wang, Y. Xiao, F. R. Fronczek, M. Xue, Y. Cui and G. Qian, *Angew. Chem.*, 2009, **121**, 508–511.
137. X. Q. Zhao, B. Zhao, W. Shi and P. Cheng, *CrystEngComm*, 2009, **11**, 1261–1269.
138. B. Zhao, X. Y. Chen, Z. Chen, W. Shi, P. Cheng, S. P. Yan and D. Z. Liao, *Chem. Commun.*, 2009, 3113–3115.

139. B. Zhao, X. Y. Chen, P. Cheng, D. Z. Liao, S. P. Yan and Z. H. Jiang, *J. Am. Chem. Soc.*, 2004, **126**, 15394–15395.
140. H. Xu, Y. Xiao, X. Rao, Z. Dou, W. Li, Y. Cui, Z. Wang and G. Qian, *J. Alloys Compd.*, 2011, **509**, 2552–2554.
141. K. L. Wong, G. L. Law, Y. Y. Yang and W. T. Wong, *Adv. Mater.*, 2006, **18**, 1051–1054.
142. B. Chen, L. Wang, F. Zapata, G. Qian and E. B. Lobkovsky, *J. Am. Chem. Soc.*, 2008, **130**, 6718–6719.
143. Y. W. Lin, B. R. Jian, S. C. Huang, C. H. Huang and K. F. Hsu, *Inorg. Chem.*, 2010, **49**, 2316–2324.
144. J. An, C. M. Shade, D. A. Chengelis-Czegan, S. Petoud and N. L. Rosi, *J. Am. Chem. Soc.*, 2011, **133**, 1220–1223.
145. B. V. Harbuzaru, A. Corma, F. Rey, P. Atienzar, J. L. Jordá, H. García, D. Ananias, L. D. Carlos and J. Rocha, *Angew. Chem., Int. Ed.*, 2008, **47**, 1080–1083.
146. A. Lan, K. Li, H. Wu, D. H. Olson, T. J. Emge, W. Ki, M. Hong and J. Li, *Angew. Chem.*, 2009, **121**, 2370–2374.
147. H. Guo, Y. Zhu, S. Qiu, A. J. Lercher and H. Zhang, *Adv. Mater.*, 2010, **22**, 4190–4192.
148. K. Liu, H. You, Y. Zheng, G. Jia, Y. Song, Y. Huang, M. Yang, J. Jia, N. Guo and H. Zhang, *J. Mater. Chem.*, 2010, **20**, 3272–3279.
149. Y. Y. Jiang, S. K. Ren, J. P. Ma, Q. K. Liu and Y. Bin Dong, *Chem. – Eur. J.*, 2009, **15**, 10742–10746.
150. K. J. Wu, C. Wu, M. Fang, B. Ding, P. P. Liu, M. X. Zhou, Z. Y. Gong, D. L. Ma and C. H. Leung, *TrAC, Trends Anal. Chem.*, 2021, **143**, 116384.
151. C. Liu, J. Li and H. Pang, *Coord. Chem. Rev.*, 2020, **410**, 213222.
152. N. Kajal, V. Singh, R. Gupta and S. Gautam, *Environ. Res.*, 2021, **204**, 112320.
153. S. Sundriyal, H. Kaur, S. K. Bhardwaj, S. Mishra, K. H. Kim and A. Deep, *Coord. Chem. Rev.*, 2018, **369**, 15–38.
154. L. Wang, H. Xu, J. Gao, J. Yao and Q. Zhang, *Coord. Chem. Rev.*, 2019, **398**, 213016.
155. J. Song, M. Huang, X. Lin, S. F. Y. Li, N. Jiang, Y. Liu, H. Guo and Y. Li, *Chem. Eng. J.*, 2022, **427**, 130913.
156. M. Lu, Y. Deng, Y. Luo, J. Lv, T. Li, J. Xu, S. Chen and J. Wang, *Anal. Chem.*, 2019, **91**, 88.
157. E. Mahmoudi, H. Fakhri, A. Hajian, A. Afkhami and H. Bagheri, *Bioelectrochemistry*, 2019, **130**, 107348.
158. Z. Lu, J. Zhong, Y. Zhang, M. Sun, P. Zou, H. Du, X. Wang, H. Rao and Y. Wang, *J. Alloys Compd.*, 2021, **858**, 157701.
159. C. Liu, X. Bo and L. Guo, *Sens. Actuators, B*, 2019, **297**, 126741.
160. N. R. Jalal, T. Madrakian, A. Afkhami and A. Ghoorchian, *ACS Appl. Mater. Interfaces*, 2020, **12**, 4859.
161. X. Tu, F. Gao, X. Ma, J. Zou, Y. Yu, M. Li, F. Qu, X. Huang and L. Lu, *J. Hazard. Mater.*, 2020, **396**, 122776.